



A comprehensive review of thermal enhancement techniques in microchannel heat exchangers and heat sinks

Akash Dwivedi¹ · Mohammad Mohsin Khan¹  · Harveer Singh Pali¹

Received: 22 May 2023 / Accepted: 30 July 2023 / Published online: 28 September 2023
© Akadémiai Kiadó, Budapest, Hungary 2023

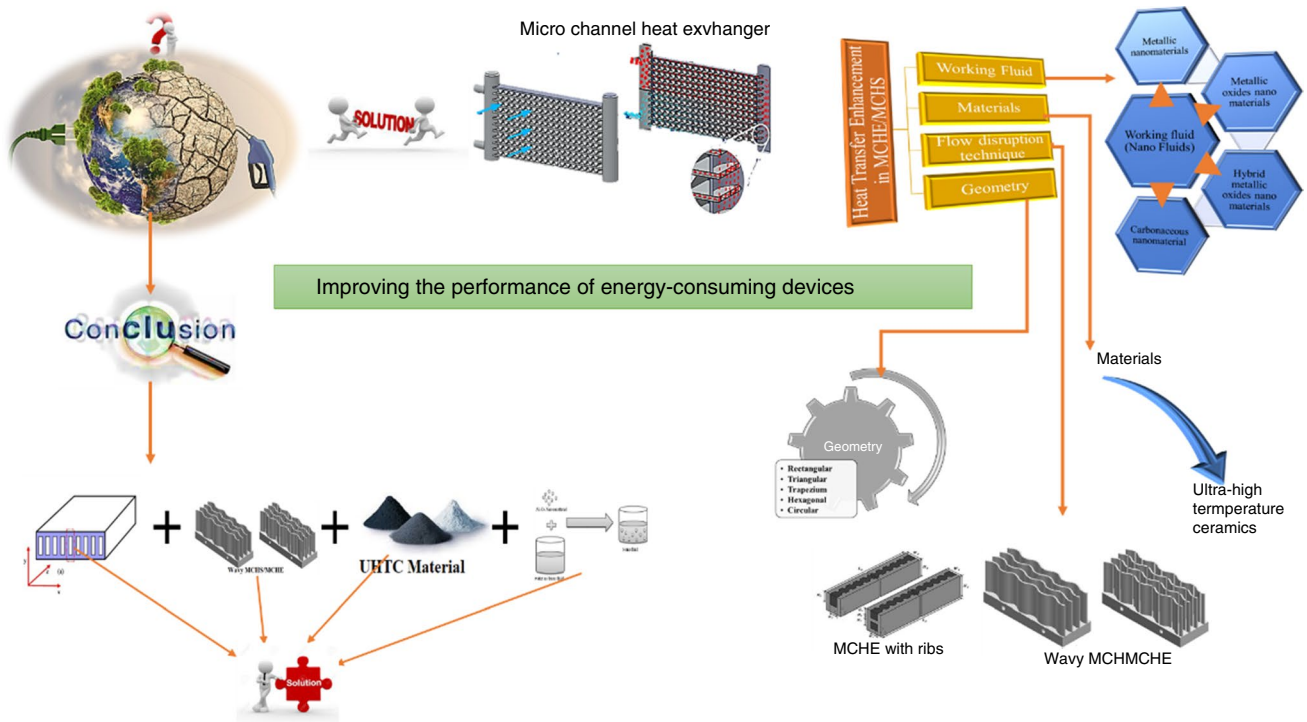
Abstract

A novel framework has been employed in various contemporary studies, to enhance heat transfer in heat exchangers through microchannels. A microchannel heat exchanger (MCHE) is a miniature heat exchanger that can address issues such as rapid increases in heat flux in small spaces, storage space constraints, and the need for compact, lightweight heat exchangers. Four perspectives were used in the qualitative literature analysis: working fluid, flow disruption, microchannel material, and microchannel cross section. The findings revealed that various working fluids (air, water, refrigerants, oil, and nanofluids) are employed in microchannel heat exchangers (MCHE) and microchannel heat sinks (MCHS); however, almost all studies have shown that nanofluids as working fluids in microchannels exhibit better thermal behavior than other fluids. Enhanced thermal performance can be achieved by adding flow disrupters (wavy channels, ribs, dimples, and baffles). Based on several applications, various materials, including aluminum (Al), copper (Cu), silicon (Si), stainless steel, silver (Ag), and various other metals, are used for MCHE & MCHS construction. However, owing to the thermal property limitations and oxidation behavior of metallic materials researchers have used ceramic microchannels to avoid these problems. The outcomes of the present review suggest that microchannel-based applications have come a long way away, but there are still barriers to addressing the needs of heat transfer in modern industries, such as the prevalence of the use of conventional rectangular shapes, water-based working fluids, metals as construction materials, and numerical techniques. Based on a literature survey, the authors suggest that rectangular wavy microchannels made of ceramic material using Al_2O_3 -water as a nanofluid have better hydrothermal behavior than any other microchannel.

✉ Mohammad Mohsin Khan
mohsinkhan@nitsri.ac.in

¹ Mechanical Engineering Department, National Institute of Technology, Srinagar, India

Graphical abstract



Keywords Microchannel heat sink · Microchannel heat exchanger · Nanofluid · Flow disruption · Wavy channels · Ceramics

Abbreviations

Ag	Silver	LWC	Longitudinal wavy channel
AlN	Aluminum nitride	MCHE	Microchannel heat exchanger
Al ₂ O ₃	Aluminum oxide	MCHS	Microchannel heat sink
Au	Gold	MWCNTs	Multiwall carbon nanotubes
Bi ₂ O ₃	Bismuth oxide	Nu	Nusselt number
BR	Bidirectional ribs	Re	Reynold number
BTR	Backward triangular ribs	SCR	Semicircular ribs
CCZ-HS	Cross-cutting zigzag heat sink	SCR	Sinusoidal cavities and rectangular ribs
CF	Carbon fluoride	SER	Semi elliptical ribs
CHF	Critical heat flux	SiC	Silicon carbide
CNT	Carbon nanotubes	SiO ₂	Silicon dioxide
CZ-HS	Continuous zigzag heat sink	SOCR	Secondary oblique channels rectangular ribs
Cu	Copper	SRC	Straight rectangular channel
CuO	Copper oxide	SR	Spanwise ribs
D _h	Hydraulic diameter	TGMCHS	Triangular groove microchannel heat sink
DI	Deionized	TiO ₂	Titanium dioxide
Fe ₃ O ₄	Ferrous oxide	TWC	Transversal microchannel
Fe	Iron	VR	Vertical ribs
Hf	Hafnium	ZnO	Zinc oxide
HVAC	Heat ventilated and air conditioning	ZrB ₂	Zirconium diboride
H ₂ O	Water		
IMCHS	Interrupted microchannel heat sink		

Introduction

The major problems in the ongoing decade are the conservation of energy and search for alternative energy sources. In the coming decades, it is anticipated that conventional energy sources will be depleted because of their ongoing use. To overcome these difficulties, some researchers have focused on substituting renewable energy sources with conventional ones. By contrast, other researchers have focused on using creative approaches to improve the energy performance of devices. Research on the development of energy-efficient devices has resulted in numerous subfields. Among the numerous methods, miniaturization of conventional devices is one. Several industries rely on heat exchangers and use conventional heat exchangers with a high thermal resistance and low efficiency. Therefore, the development of heat exchangers is required to lower thermal resistance, boost convective heat transfer, and enhance efficiency. A heat exchanger is designed to transfer heat from one fluid to another without losing heat to the surrounding environment. Two significant phenomena occur in a heat exchanger: fluid movement in passages and the transfer of energy between the channel walls and fluids. Hence, these devices can be made more efficient by enhancing the performances of these two phenomena. Because the heat transfer rate is dependent on the ratio of the surface area to the volume, smaller channel dimensions result in a higher heat transfer coefficient. Conventional heat exchangers employ tubes with a diameter of ≥ 6 mm; however, microchannels with a size of ≤ 1 mm are the next phase in the development of heat sink and heat exchangers. Owing to their high rate of heat transfer potential and lightweight, as well as their ability to save energy, space, and materials compared with conventional heat exchangers, this field of study is the subject of significant attention and analysis.

Microchannels are defined as narrow flow tubes of size 1 mm or less, that allow for heat transfer surface densities of $10,000 \text{ m}^2 \text{ m}^{-3}$ or higher [1], in contrast to conventional channels with a surface density of $700 \text{ m}^2 \text{ m}^{-3}$. Micro and minichannels differ from normal channels in terms of the channel hydraulic diameter (D_h). The classification methods proposed by Mehendafe et al. [2] and Kandlikar et al. [3], the

latter of which is becoming increasingly popular, are typically adopted. Table 1 lists the terminology used by these authors.

The amount of heat that can flow through the microchannels depends on the surface area which can facilitate heat transfer, which is determined by the hydraulic diameter (D_h) of the channel. By contrast, the flow rate is determined by the cross-sectional area of the channel, which is proportional to D_h^2 . Therefore, as D_h decreases, the surface-area-to-volume ratio increases, indicating that the surface area of the channel relative to its volume increases. The flow within the microchannels is typically laminar, and the local heat transfer coefficient varies inversely with D_h . Consequently, a decrease in D_h was necessary to enhance the heat transfer coefficient. Tuckerman and Pease [4] suggested an initial study of the MCHS approximately 40 years ago. They assumed that reducing the D_h of the channel would increase heat transfer. This invention has strengthened the electronics industry, which has dealt with difficulties such as high heat dissipation in compact areas. Kandlikar et al. [5] studied the thermohydraulic performance of minichannels and microchannels in their literature. In the initial stages of microchannel development, there were significantly fewer publications. However, microchannels have slowly become the most crucial field of research, as shown in Fig. 1 (references are taken as per Scopos).

Microchannel heat sink (MCHS) and its applications

A heat sink is a device that uses extended surfaces to collect heat from a source and effectively disperses it into the environment effectively as shown in Fig. 2. The capacity of traditional channel heat sinks to dissipate heat is limited even with the use of forced convective cooling. However, as technology has progressed, concerns regarding high heat dissipation in small spaces have increased. Micro- and minichannels have provided appropriate solutions to meet these objectives. Heat sinks are classified as passive, active, liquid-cooled, or phase-change heat sinks depending on the cooling technology used for a specific application as shown in Table 2. The MCHS is particularly effective for removing high heat fluxes and maintaining electronic component temperatures within

Table 1 Channel taxonomy based on hydraulic diameter

Mehendafe et al. [2]	Hydraulic diameter	Kandlikar and Grande[3]	Hydraulic diameter
Traditional channels	> 6 mm	Traditional channels	> 3 mm
Compact passages	1 mm to ≤ 6 mm	Minichannels	200 μm to ≤ 3 mm
Mesochannels	100 μm to ≤ 1 mm	Microchannels	10 μm to ≤ 200 μm
Microchannels	1 μm to ≤ 100 μm	Transitional channels	0:1 μm to ≤ 10 μm
		Molecular nanochannels	$\leq 0:1$ μm

Publications in microchannel heat exchangers

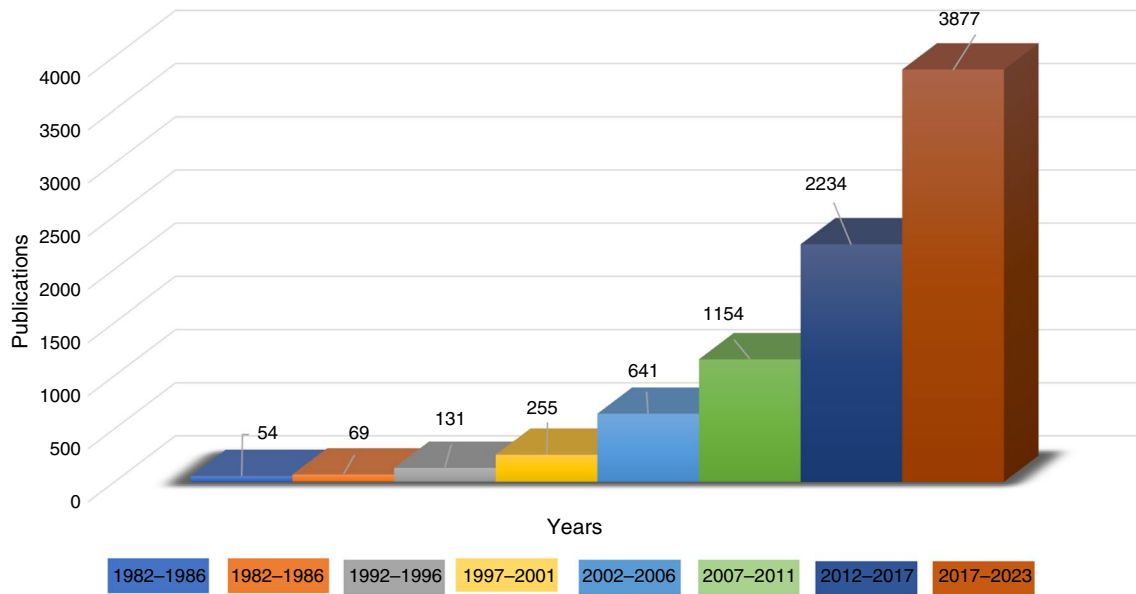


Fig. 1 Publications on microchannel heat exchanger as per Scopus

Fig. 2 MCHS design & boundary parameters. (a) Front view (b) detailed view

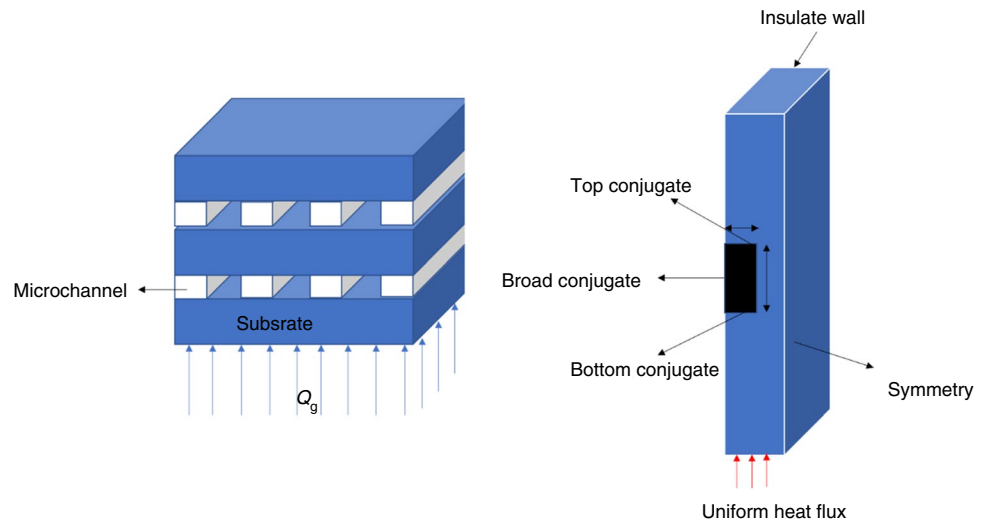


Table 2 Classification of heat sinks

Heat sink category				
	Active	Passive	Liquid cooling	Phase change cooling
Applications	High power intensity uses	Natural convection systems, simple power intensity uses	High power intensity uses	For high power output
Benefits	Heat sink with fan, large heat dissolution capacity	Consumer friendly, economical	High heat dissolution capacity compared to active and passive	Heat dispersed equally
Drawback	Expensive	Limited power dissolution capacity	Complicated & expensive	Expensive, complex, and requires more area
Examples	Fan, fins, heat sink	Metal plate	Liquid cold plate	Vapor firmness phase

acceptable limits. Unlike regular channels, microchannels can dissipate power densities up to 1000 W cm^{-2} , whereas conventional channels can only dissipate heat fluxes up to 20 W cm^{-2} . Xiang et al. [6] conducted a series of comparative experiments to assess the heat transfer capabilities of a microchannel heat sink in comparison with a conventional metal solid heat sink. The results indicate that the microchannel heat sink outperforms the conventional metal solid heat sink in terms of heat dissipation performance. This makes them an excellent choice for applications involving high power LEDs. To cool the electronic devices, Xiong et al. [7] proposed the use of microchannels as liquid-cooled thermospreaders linked to gas-cooled heat sinks. In addition to integrated circuits, these channels have been used in many other applications. Micropumps, microturbines, micromotors, microvalves, and microreactors are devices that are based on this technology [8]. Additionally, micro-scale development has spawned a new field of microfluidics.

Micro-/minichannel heat exchangers and applications

With respect to heat exchangers, Little et al. [9] were the first to realize the possibilities of micro- and minichannels. The authors suggested that these narrow channels could be used in small-scale Joule–Thomson refrigeration systems. Swift et al. [10] were the first to submit a patent application for the manufacturing process of microchannel heat exchangers (MCHE) with cross-flow. These heat exchangers can be used as energy-efficient alternatives to conventional HVAC (heating, ventilation, and air conditioning) systems. The additional benefit of MCHE in these systems is that they consume less refrigerant and have a greater overall system efficiency. However, owing to their high manufacturing costs and lack of “precise performance prediction tools,” their commercial use is limited. MCHE, on the other hand, has found widespread use in refrigeration [11] and air-conditioning systems [12]. window air conditioning [13], split air conditioners [14], chillers, air-cooled ammonia condensers [15], vapor compression refrigeration systems [16], and heat pumps [17] are just a few examples. A schematic of the various MCHE types is shown in Fig. 3, along with information about their uses, types, construction materials, and fabrication methods.

Classification of microchannel design

Numerous attempts have been made to reduce the thermal resistance of MCHS and enhance their heat transfer ability. Steinke and Kandlikar [5] examined the use of

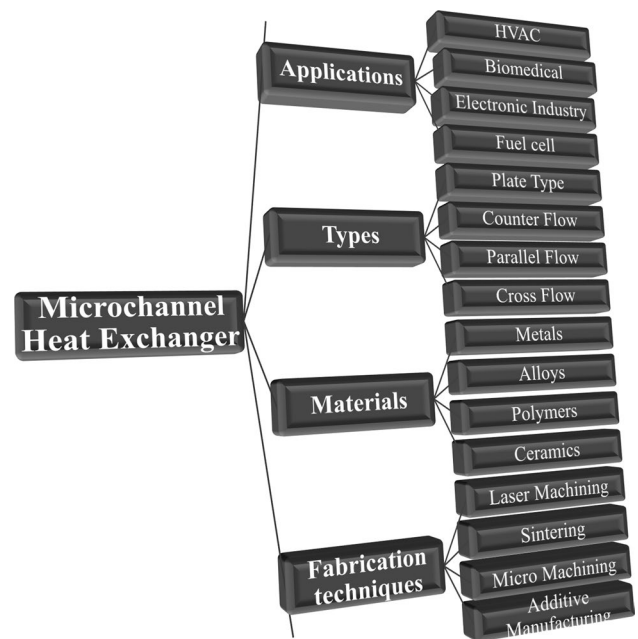


Fig. 3 represent the classification of MCHE

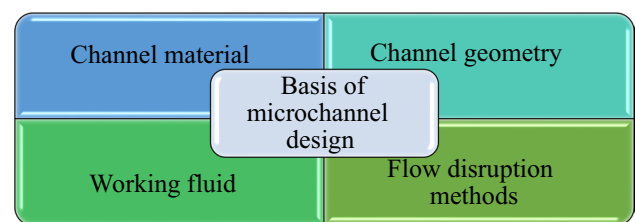


Fig. 4 Heat transfer enhancement methods in microchannel design

passive and active strategies to improve the thermal properties of mini- and microchannels. Active methods for improving the heat transfer rely on additional vibrational, magnetic, and electric flux forces. In contrast to active techniques, which often depend on external factors, passive techniques enhance heat transfer by means such as flow disruption, changing the geometry, and altering the working fluid of the heat sink. In addition, they performed a comprehensive analysis and assessed the feasibility of using these methodologies in novel MCHS applications. This review discusses the essential heat transfer enhancement methods used in microchannel design, as shown in Fig. 4. Microchannel designs can be categorized based on several factors, such as the types of working fluids utilized in microchannels, materials utilized to construct microchannels, techniques employed in microchannels to disrupt flow to improve heat transfer, and microchannel geometries.

Working fluid

Microchannels in the twentieth century used various working fluids. The most frequently used fluid is water, followed by air and various gases. Other fluids include liquid and gaseous nitrogen, common refrigerants, alcohol, and lubricants. Water has been commonly employed as the primary working fluid in earlier research; however, its limited thermal conductivity in comparison with metals restricts its applicability in microchannels. Nanofluids have received considerable attention over the last two decades because of their exceptional thermophysical properties. Owing to their exceptional thermal properties, nanofluids can be used in various applications such as solar energy devices, aerospace, the automobile industry, electronic devices, medical applications, and manufacturing sector as shown in Fig. 5.

Nanofluids

A nanofluid is a mixture of a base fluid and suspended solid particles on a nanometer scale. Suspending tiny solid particles in energy-transfer fluids can significantly improve their thermal conductivity and provide a cost-effective novel technique for improving their thermal characteristics. The

concept of “nanofluid” was coined by Choi [18] to describe a mixture of base fluids such as water, glycerine, ethylene glycol, and oil with nanoparticles. This combination resulted in a significant enhancement of the thermal characteristics of the fluid. Standard fluids such as water and ethylene glycol have low thermal conductivities, but adding solid particles to the fluid can enhance the thermal conductivity because solid materials typically have a higher thermal conductivity than fluids. It is possible to employ metallic or nonmetallic solid particles. However, large micro- and macro-sized particles may block flow channels and have poor stability, making their use unjustifiable. Table 3 lists the metallic, metallic oxide, and carbonaceous materials and their corresponding thermal conductivities. Compared to commonly used heat transfer fluids such as water, ethylene glycol, and various oils, these materials exhibit significantly higher thermal conductivities.

Researchers have conducted several studies on the use of nanofluid in MCHS, necessitating a review of prior and current research to identify and carry out future research. The most important criterion before using a nanomaterial as a nanofluid in a microchannel is the material selection. The possible factors for selecting a nanomaterial for use in the creation of nanofluids for heat transfer in microchannels are the thermal characteristics, chemical stability, safety,

Fig. 5 Various applications of nanofluids

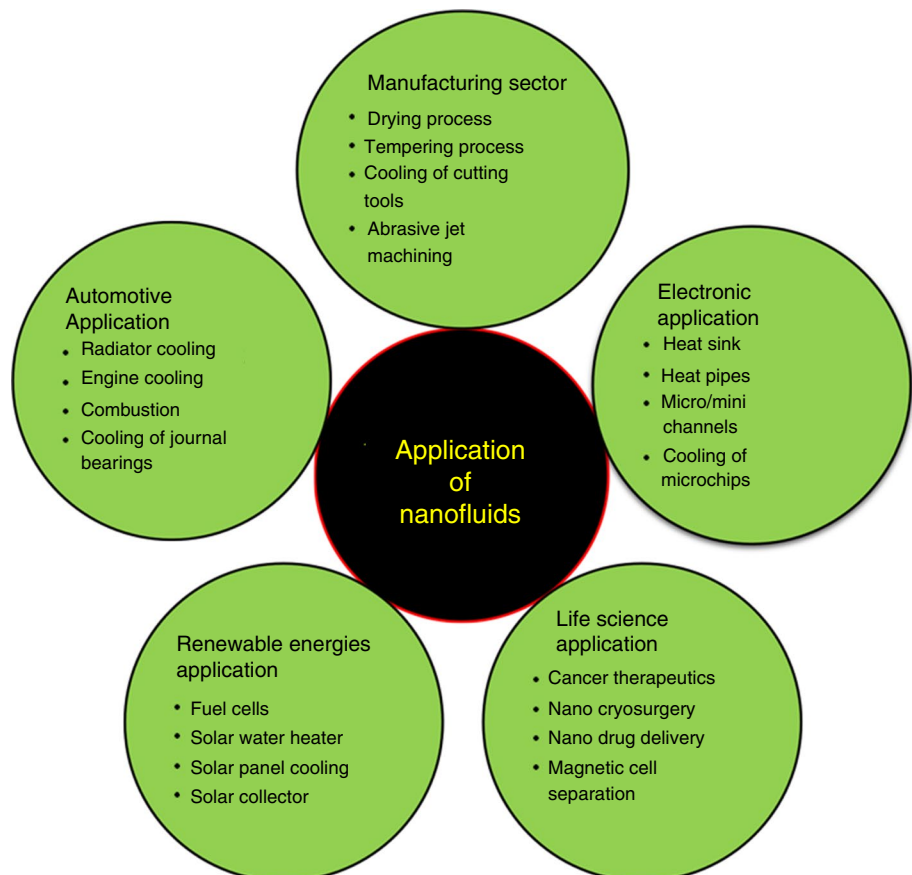


Table 3 Thermal conductivity of the various base fluid and base materials of nanofluid

Types	Material	Thermal conductivity/W m ⁻¹ K ⁻¹
Liquids	Water	0.613
	Ethylene glycol	0.253
	Engine oil	0.15
Nonmetallic solids	Titanium	23
	Silicon	148
	Alumina	40.0
	Sodium	72.3
Metals	Copper	401
	Aluminum	237
	Zinc	112.2
	Nickel	67
	Ferrous	80
Metal oxide	Al ₂ O ₃	40
	ZnO	13
	CuO	20
	SiO ₂	1.1–1.4
	TiO ₂	4.8
	Fe ₃ O ₄	17.65
Carbonaceous material	Diamond	≥ 1500
	CNT	≥ 3000

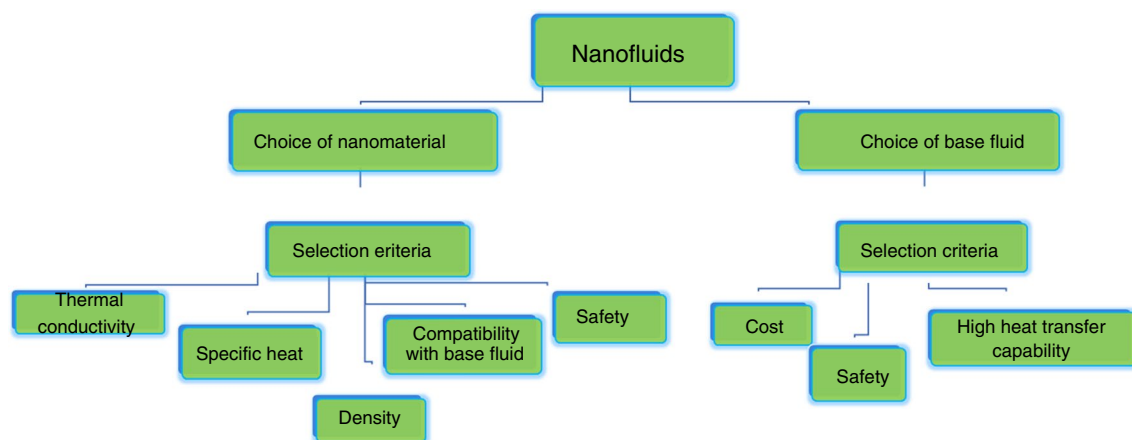
compatibility with the base fluid, affordability, and accessibility [19, 20]. Figure 6 presents an overview of the aspects to be considered when selecting a nanomaterial for nanofluid creation.

Advances in nanofluid preparation

- *Synthesis Techniques* Different techniques have been developed to create stable nanofluids with controlled particle dispersion. These include chemical processes, physical processes (such as milling or laser ablation), and more contemporary approaches, such as electrochemical synthesis and green synthesis.
- *Characterization Techniques* Techniques like transmission electron microscopy (TEM), dynamic light scattering (DLS), and X-ray diffraction (XRD) were used to obtain a clear picture of the size, shape, distribution, and physical characteristics of the nanoparticles. These approaches aid in understanding the behavior and stability of nanofluids.
- *Surface Modification* Nanoparticles can be functionalized via surface modification methods, improving their dispersion stability and compatibility with the base fluid. Surfactant coating, polymer grafting, or chemical processes can be used to modify the surfaces.
- *Stability Enhancement* Researchers are working to find ways to make nanofluid more stable over time. The most common methods are the use of stabilizing agents, magnetic fields, and external fields such as ultrasound and electric fields to prevent nanoparticle agglomeration and sedimentation.

Effect of nanomaterial on the stability of nanofluids

Nanofluid are suspensions that remain in a stable equilibrium state when subjected to different forces, such as van der Waals, electrostatic, and gravitational forces. The ability to maintain this state is known as the stability of the nanofluid, and this ability of nanofluids is a crucial

**Fig. 6** Classification of nanofluids based on selection criteria

characteristic to consider when employing in many applications, including MCHS and MCHE. The stability of nanofluids can be influenced by several factors, including the choice of nanomaterial, base fluid properties, nanomaterial concentration, surface chemistry, and temperature [21, 22]. The stability of a nanofluid can be evaluated by various methods, such as:

- *Zeta potential analysis* The zeta potential analysis evaluates the stability of nanofluids through the observation of the electrophoretic behavior of the fluid. Higher absolute zeta potential values (either positive or negative) indicate greater repulsion between the particles, leading to enhanced stability.
- *Electron microscopy methods* The particle size distribution of the nanofluid was measured using transmission electron microscopy (TEM) or scanning electron microscopy (SEM). SEM & TEM are widely used by researchers to investigate particle shape, size, and aggregation, as shown in Fig. 7.
- *Sedimentation photograph capturing method* In this method, the volume of agglomerated nanoparticles in a nanofluid is observed under an external force. This was done by placing a sample of the prepared nanofluid in a transparent glass vial; and the formation of sediments was observed by capturing photographs of the vial at equal intervals of time using a camera. The captured images were then compared to analyze the stability of the nanofluid. Thus, the characterized nanofluid is consid-

ered stable when the particle size and dispersity remain constant over time.

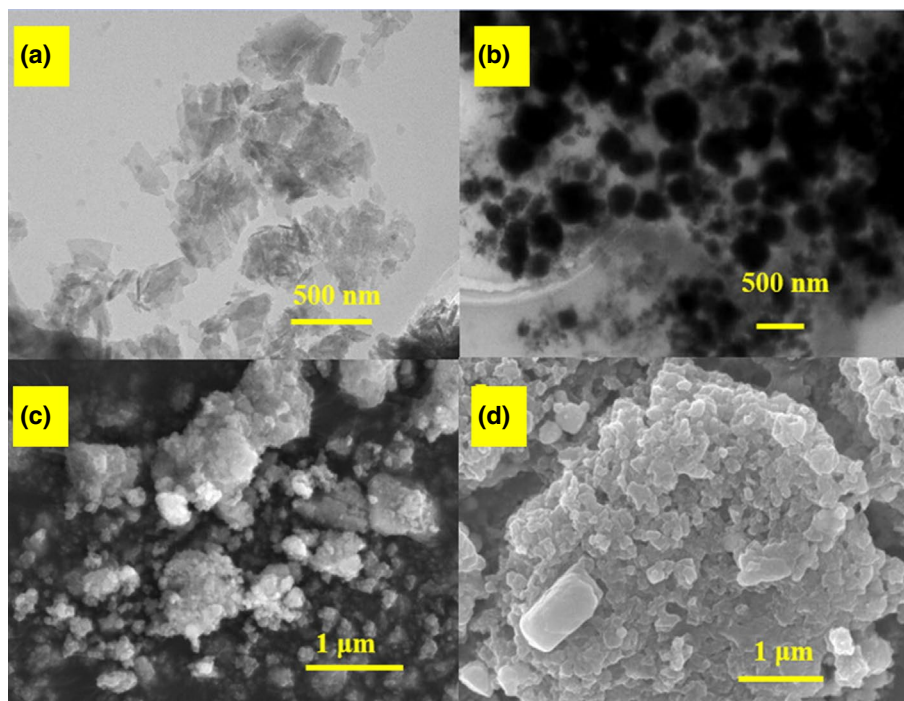
- *Centrifugation method* In this method, nanofluid sedimentation was performed using a dispersion analyzer centrifuge.

Achieving long-term stability in nanofluids is crucial for their practical application, as it ensures consistent performance and prevents issues such as clogging in microchannels or sedimentation during storage. Researchers continue to explore methods for enhancing and maintaining the stability of nanofluids to maximize their efficacy in heat transfer and other relevant applications. Various methods can be used to improve the stability are:

Surfactant stabilization Surfactants are chemical compounds that can be added to nanofluids to provide electrostatic or steric stabilization. They form a protective layer around the nanoparticles, preventing agglomeration. Surfactants can be anionic, cationic, or nonionic, and their selection depends on the nature of the nanoparticles and base fluid.

Surface modification Nanoparticle surfaces can be modified to enhance their stability. Surface functionalization involves attaching molecules or polymers to the nanoparticle surface, which can provide repulsive forces between the particles, reducing agglomeration. Functionalization can be achieved through various methods, such as silane coupling agents, polymer coating, or ligand exchange.

Fig. 7 SEM and TEM image
Ref. [23]



pH adjustment Changing the pH of the nanofluid can affect its stability by altering the surface charge of the nanoparticles. The choice of pH adjustment depends on the nanoparticle material and surface chemistry. By adjusting the pH, repulsive forces can be enhanced, hindering agglomeration.

Ultrasonication Ultrasonication involves subjecting a nanofluid to high-frequency sound waves, typically in the range of 20–100 kHz. The acoustic cavitation generated during ultrasonication helps disperse and deagglomerate nanoparticles. This process breaks down the large agglomerates into smaller particles, enhancing their stability.

Mechanical stirring Mechanical stirring or mixing with the nanofluid can help distribute nanoparticles evenly throughout the base fluid. Agitation disrupts agglomerates and promotes the uniform dispersion of nanoparticles. The intensity and duration of stirring should be optimized to prevent excessive energy input, which can lead to excessive heating.

Characterization of nanofluids

The process of determining and understanding the properties, characteristics, and behavior is referred to as characterization. The characterization of nanofluids involves measuring various physical and chemical properties such as thermal conductivity, viscosity, density, surface tension, composition, surface morphology, and stability. It is crucial to understand these properties as they affect the thermo-fluidic behavior of nanofluids in microchannels. Some common methods used for nanofluid characterization are as follows:

1. Scanning electron microscopy (SEM)—is used to study the distribution of materials on a surface.
2. SEM & EDS—is used to measure the elemental composition in a sample.
3. Transmission electron microscopy (TEM)—which is used to visualize the smallest structures in matter, produces high-resolution images.
4. FTIR analysis—was used to identify unknown compounds, determine the purity of the sample, and monitor the chemical reactions in real-time.
5. Transient hot wire—determines the thermal conductivity
6. Laser flash method—determines the thermal conductivity
7. Rheometer—was used to study fluid properties such as dynamic viscosity, flow behavior (Newtonian/non-Newtonian).
8. DSC—To measure the specific heat capacity of the nanofluid as a function of temperature.

9. Oscillation method—is used to measure the density of nanofluid.
10. Pendant drop method—is used to study the surface tension of nanofluids, which is a property of the interface between the fluid and surrounding air or another medium.

Therefore, characterization of nanofluids is essential for understanding their behavior. Table 4 presents various characterizations of the nanofluids and instruments used for their measurements.

Base working fluid used in microchannel

Water, oils, glycols, and glycol–water combinations are commonly used as base fluids to create nanofluids. Figure 8 shows that among the different base fluids, water-based nanofluids have received the most attention from researchers, likely because of their lower cost and higher thermal conductivity. Owing to their potential as high heat transfer fluids in microchannels, glycol-based nanofluids have also attracted attention.

Nanomaterial used for nanofluid formation

The nanoparticles commonly used for nanofluid creation are metals, metal oxides, carbonaceous materials, and hybrid nanoparticles. Figure 9 shows the distribution of publications on nanofluids employing various nanomaterials in microchannels. Although metal oxides exhibit lower thermal conductivities than metals, they appear to be the most suitable option for creating nanofluids. This is because metal oxides are chemically stable and are resistant to oxidation. Moreover, certain metal oxides have a lower density than their corresponding metals, which could lead to fewer particle-settling problems in nanofluid formulations. Owing to its high thermal conductivity and low density, alumina is widely used as a metal oxide for nanofluid formation. Based on the nanomaterial used for nanofluid creation in the present study. The authors reviewed all the journals on nanofluids and categorized them into four main types.

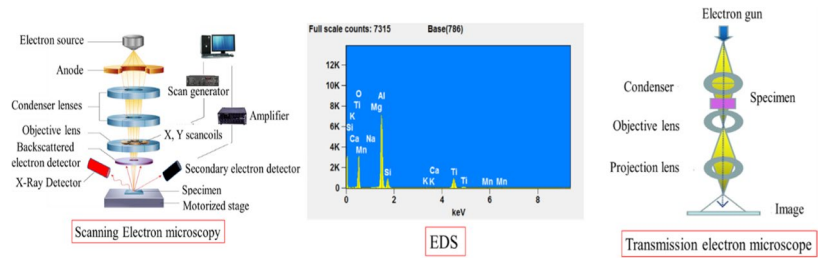
(a) Nanofluids used in various microchannel geometries suspended with metallic nanoparticles.

Metallic nanofluids (e.g., Ag, Cu, Fe, Au, etc.) generate higher effective thermal conductivity values. Therefore, various researchers have focused on using metallic nanomaterial for nanofluid creation, as presented in Table 5. Mghari et al. [24] conducted a numerical analysis of the heat transfer in a single horizontal smooth square tube. According to the findings of the research, either elevating the mass flux from 80 to 110 kg m⁻²-s or increasing the concentration of copper

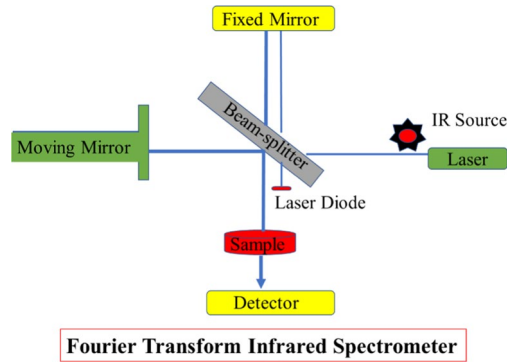
Table 4 Characterizations techniques of nanofluids

Characterization of Nanofluids

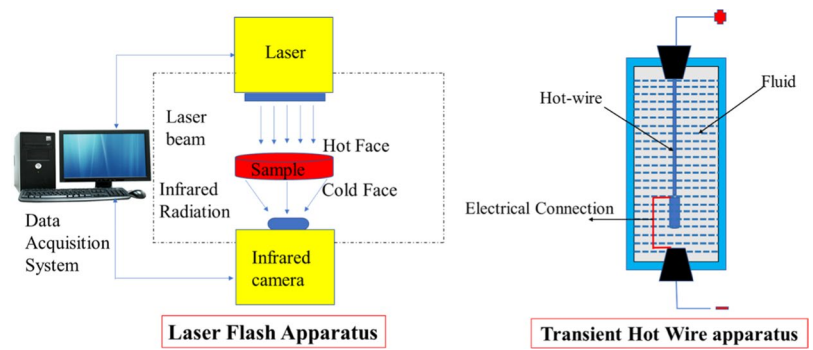
Surface morphology



Composition



Thermal conductivity



Rheological properties

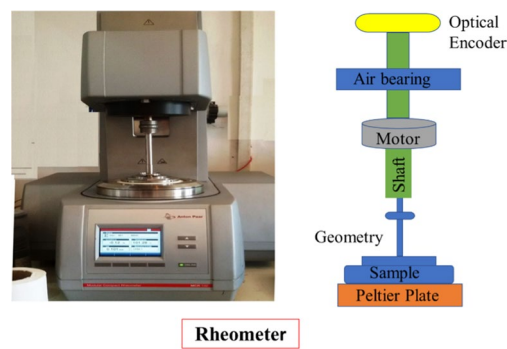
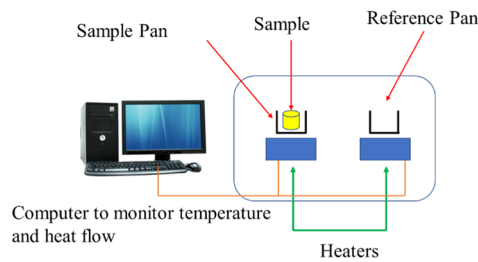


Table 4 (continued)

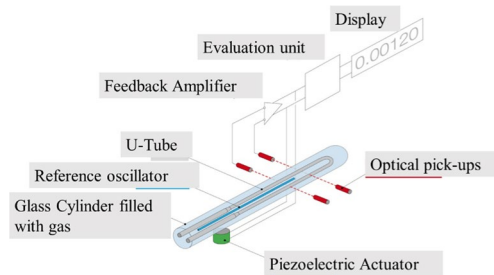
Characterization of Nanofluids

Specific heat



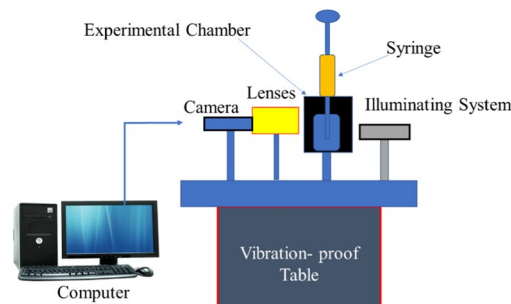
Differential Scanning Calorimeter

Density



Density meter

Surface tension



Pendant Drop Apparatus

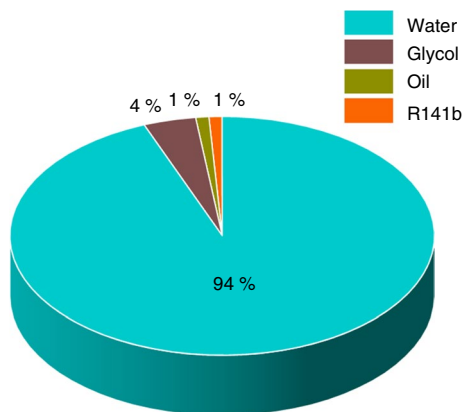


Fig. 8 Base fluid use in microchannels for nanofluids formation

nanoparticles by 5% has the potential to increase the heat transfer coefficient by 20%.

Abbassi and Aghanajafi [25] examined the incorporation of Cu nanoparticles into MCHS. The results of their research showed that employing a nanofluid significantly improved the heat transfer in the MCHS, and this advantage became even greater as the Re and particle concentration increased. Additionally, they demonstrated that if the flow regime transitions into the turbulent domain, the enhancement in heat transfer could be greatly amplified.

Diao et al. [26] analyzed the performance of a micro-channel surface in a vapor chamber using Cu-R141b as the working fluid. The authors recommended that with a volume concentration of 0.001–0.01 percent, R141b-based Cu nanofluids may enhance the thermal performance of microchannel surfaces, especially at lower operating pressures.

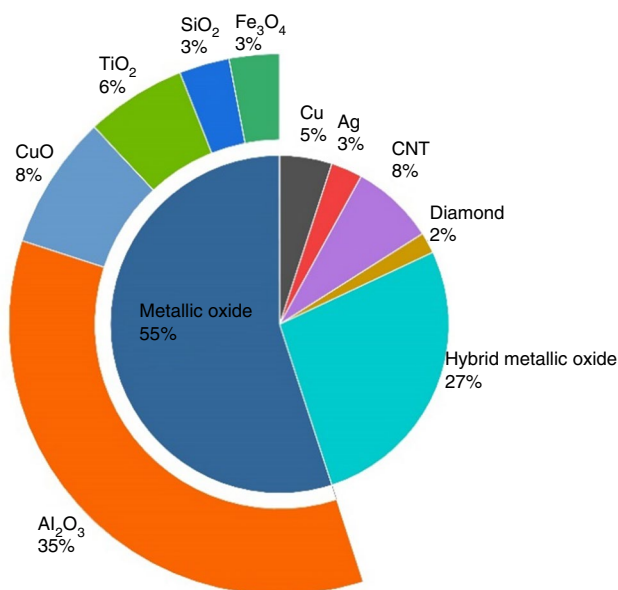


Fig. 9 Nanofluids used in various microchannel geometries

Boudouh et al. [27] analyzed the convective boiling heat transfer in a vertical rectangular channel using copper–water nanofluids and deionized water. They found that in comparison with the temperature and pressure of the base fluid, the Cu–water nanofluid exhibited a lower surface temperature and local heat flux at the same flow rate.

Using porous media and the least square method, Hatami and Ganji [28] investigated the thermal performance of a MCHS employing a nanofluid composed of copper and water. They observed that raising the volume fraction of nanoparticles encouraged Brownian motion and facilitated greater heat transfer.

Simsek et al. [29] employed suspensions of silver nanowires to enhance thermal performance in a MCHS for the first time. According to the outcomes, the utilization of silver nanowire suspensions in MCHS could lead to a rise in heat transfer coefficient of up to 56%, while causing only a minor increment in pumping power.

Tehrani et al. [30] conducted a numerical analysis on flow and heat transfer of an Ag–water nanofluid under varying heat flux, while considering different volume concentrations and Hartmann numbers. They suggested that because the Re of nanofluids inside microchannels is often low, “utilizing a higher volume fraction to enhance the Nusselt number (Nu) would be counterproductive in micro and nanoflows.” Shahsavari et al. [31] conducted a numerical investigation to enhance the performance of a liquid-cooled heat sink. In this study, a water/silver nanofluid was used as the coolant. The researchers focused on two operational variables: nanoparticle concentration and Reynolds number. They also examined the impact of a structural parameter, specifically

rifling the inlet tube of the coolant. The results revealed that the overall hydrothermal performance of the heat sink with a rifled inlet was 1.073–1.541 times higher compared to the heat sink with a plain inlet.

Table 5 indicates that copper and silver are the most commonly used nanomaterials for preparing working fluids in research, likely due to their high thermal conductivity compared to other metallic materials. Based on the research on metallic nanofluids, it can be concluded that increasing particle concentration results in nearly a 50% improvement in heat transfer in the microchannel in most cases. However, this may also cause an increase in pressure drop.

(b) Nanofluids used in various microchannel geometries suspended with metallic oxides nanoparticles

Despite their poorer thermal conductivities than those of metals, metal oxides have been frequently employed in the formulation of nanofluids. Metal oxides (e.g., Al₂O₃, CuO, TiO₂, SiO₂, etc.) have several benefits over metal nanoparticles, including oxidation resistance and chemical stability. Furthermore, some metal oxides have lower densities than metals, resulting in less sedimentation when they are used in nanofluid formulations. This concept is a popular research topic because it is a viable solution for satisfying the temperature management requirements of the MCHS and MCHE. Tables 6–11 represent the literature on metallic oxide nanoparticles for the formation of nanofluids used in various microchannel geometries.

The study conducted by Bhattacharya et al. [38] on the heat transfer properties of an Al₂O₃–H₂O nanofluid flowing through a rectangular MCHS showed that an increase in nanoparticle concentration resulted in a more pronounced improvement in MCHS performance with the use of the nanofluid.

In a study conducted by Ali et al. [39], the thermal performance of a circular MCHS was evaluated in the range of $100 \leq Re \leq 350$, using swirl flow and nanofluid. The coolant was a water–Al₂O₃ nanofluid with nanoparticle volume fractions ranging from 0 to 3%. The results indicated that the MCHS with swirl flow and maximum nanoparticle volume fraction had the lowest thermal resistance and contact temperature.

Meanwhile, Heidarshenas et al. [40] utilized an ionic liquid–Al₂O₃ nanofluid to enhance heat transfer in a cylindrical MCHS. Their findings showed that the use of ionic liquid–Al₂O₃ nanofluid increased the Nusselt number by up to 40%.

The thermal performance of a trapezoidal microchannel was studied by Li and Kleinstreuer [41] using pure water and CuO–water with volume fractions of 1% and 4%, respectively. They found that with a modest increase in pumping

Table 5 Effect of metallic nanomaterial in MCHS and MCHE on various geometry

S. no.	Study type	Geometry	Reynolds number	Nanoparticle	Particle size/hm	Particle conc./%	Max HT. gain/%	Outcomes	Ref.
1	Experimental	Rectangular	-	Cu	20	0.001-0.1	50	The impact of nanofluid on thermal resistance is more apparent at lower operating pressures than at higher ones	[26]
2					35	5-50 mg/L	-	The concentration of Cu nanoparticles enhances heat transfer coefficient, vapor quality, & local heat flow	[27]
3			20-71	Ag	50-100	0-0.00357	56	For all microchannel diameters, Ag-water nanofluids produce lower thermal resistance than DI water	[29]
4			< 1500		5-10	0.01-0.1	-	Both the heat transfer coefficient and the pressure drop of the (MCHS) increased as the flow rate and mass concentration of nanofluid increased	[32]
5	Numerical	Rectangular	10-200	Ag	10	0-4	-	Utilizing a higher volume fraction to enhance the Nu would be counterproductive in micro and nanoflows	[30]
6		Trapezoidal, Rectangular, Triangular	1-100		50	0-4	100	The convective heat transfer coefficient of the working fluid increases with an increase in the nanoparticle volume percentage	[33]
7		Triangular	5-500		25-75	0-4	-	The friction coefficient and pumping power do not show a significant dependency on nanoparticle diameter	[34]
8		Trapezoidal	10,000-16,000		-	0-4	-	The average Nu and convection heat transfer coefficient rise as Re rises	[35]
9		Circular	1-1000	Cu	-	2-4	-	Reducing the channel height may result in the combination of boundary layers and the loss of the entrainment effect. Thus, decreasing the channel area may not necessarily lead to an increase in total heat flux	[36]
10		Parallel Plates	< 1400	Cu, NEPCM	36	1.3-5	-	Compared to both NEPCM and water, Cu-water nanofluid exhibits a higher average heat transfer coefficient	[37]
11		Square	< 700	Cu	-	0-5	20	Enhancement of the heat transfer coefficient by 20% may be achieved by either increasing the volume percentage of Cu nanoparticles by 5% or by raising the mass flow from 80 to 110 kg m ⁻² s ⁻¹	[24]
12		Rectangular	100-2000	Cu	23	0-6	-	Transitioning to the turbulent regime of fluid flow can significantly increase the heat transfer enhancement of the nanofluid	[25]
13	Analytical	Rectangular	-	Cu	1-25	0-6	-	Increasing the volume fraction of nanoparticles results in an increase in Brownian motion, which in turn causes a decrease in the temperature differential between the coolant and the wall	[28]

Table 6 Numerical, experimental, and analytical analysis of the effect of Al_2O_3 and water base nanofluid in a rectangular cross section micro-channel

S.no.	Study type	Reynolds number	Particle size/nm	Particle Conc./%	Max. H.T gain	Outcomes	Ref.
1	Numerical	200–1200	38	0–4	–	If temperature-dependent properties are incorporated, the temperature and average shear stress on the bottom surface decrease	[47]
2		150–450	38.4	0–2	–	Compared to the constant property approach, the variable property technique results in a higher heat transfer coefficient and Nusselt number	[48]
3		< 450	–	0.5–3.5	–	Using a tear-drop dimple structure in combination with nanofluid can increase heat transfer while reducing pressure loss	[49]
4		0.025–250	–	0–2	–	The formulation of the Buongiorno model causes the incorporation of Brownian motions	[50]
5		5–300	25–100	0–2	–	Using nanoparticles with decreasing diameters and increasing the nanoparticles volume percentage increases heat transfer	[51]
6		100–400	–	0–4	12.67	Increasing either the volume percentage of nanoparticles or the aspect ratio of the fins may lead to an increase in heat transfer	[52]
7		< 500	36	1–4.5	–	The use of nanofluids as a cooling medium in electrical devices results in an increase in the power required for fluid pumping	[53]
8		200–1000	40	0.1–0.2	130	Increasing Re, increasing volume concentration and decreasing nanoparticle size all result in an increasing average Nu	[54]
9		–	–	0–5	10.93	With the increase in Knudsen number, both temperature gradient and average Nu decrease	[55]
10		100–1000	–	1–5	–	Compared to a MCHS cooled with pure water, the use of nanofluids results in a slight increase in pressure loss across the system	[56]
11		5–150	–	0–5	–	The overall increase in cooling performance of nanofluid in microchannel system becomes more effective when water is employed as base fluid	[57]
12		–	–	0–1	–	The enhanced thermal performance of nanofluid-cooled MCHS is attributed to the intake flow velocity and effective thermal conductivity of nanofluid	[58]
13		10–1000	25	0.5–1.5	–	Increasing the volume percentage of solid nanoparticles and decreasing the size of the nanoparticles can enhance heat transfer	[59]
14		120–480	29,38.4, 47	0–4	–	Pumping power and frictional entropy contribution both decreases as heat transfer entropy diminishes	[60]

Table 6 (continued)

S.no.	Study type	Reynolds number	Particle size/nm	Particle Conc./%	Max. H.T gain	Outcomes	Ref.
15		–	33	0–2	–	The effect of inertia on the temperature profile of the channel wall is negligible; however, it has a substantial impact on the temperature profile of the coolant and the overall thermal resistance	[61]
16		250	20	0–3	–	The enhancement in MCHS performance due to the utilization of nanofluid becomes increasingly noticeable with an increase in the particle concentration	[38]
17		< 1500	40	0–4	29	By applying a magnetic field, the thermal boundary layer formation is disturbed, leading to an improvement in heat transfer	[62]
18		150–700	0–2.5	–	–	Microchannel outperforms when elliptical ribs are employed instead of diamond ribs or no ribs	[63]
19		7–15	0–5	–	–	Raising the input velocity to maintain a constant Re, rather than increasing the particle concentration, is the primary way to raise the Nu for a given Re	[64]
20		5–25	–	0–4	17	The magnetic field does not influence heat transfer, but it may increase friction up to 86%	[65]
21		–	–	0–2.5	–	Heat transfer coefficient and Nu fluctuation both decreases with flow direction as the boundary layer thickness increases	[66]
22		1–100	50	0–4	350	An increase in particle volume fractions improves heat transfer & friction factor	[67]
23		–	–	0–2	8.49	The temperature of the nanofluids in the microchannel rises with the curve, contradicting the linear growth concept	[68]
24		200–1500	–	1–5	–	Throughout the channel length, there is an increase in the temperature of both the coolant and MCHS for all values of nanoparticle volume fractions	[69]
25		15,000–30,000	50	0–4	237	Fluid mixing is influenced by variations in the attack angle of the ribs and the creation of vortexes within the channel	[70]
26	Analytical	0–200	40	0–4	70	The thermal efficiency of nanoparticles may be improved by as much as 70% by lowering their diameter below the threshold value	[71]
27	Experimental	45–80	43	0.1–0.25	–	The thermal efficacy of nanofluids is quite high, which encourages the use of nanofluids in MCHS	[72]
28		–	–	0–2	–	The utilization of nanofluids in ribbed microchannels results in increased Nu and friction coefficient compared to ordinary microchannels. Additionally, this improvement is more significant with increased rib width	[73]

Table 6 (continued)

S.no.	Study type	Reynolds number	Particle size/nm	Particle Conc./%	Max. H.T gain	Outcomes	Ref.
29		–	40	0–0.2	–	Nanofluid considerably reduces flow instability without causing nanoparticle deposition	[74]
30		226–1676	33	0–2	70	A heat sink cooled by nanofluid has a higher average heat transfer coefficient compared to one cooled by water, making it superior in terms of heat dissipation performance	[75]
31		–	80	0–0.5	27	Nanofluids with higher concentrations exhibit higher thermal conductivity and viscosity	[76]
32		–	25	0.001–0.1	–	Nanoparticles in the liquid phase can significantly affect bubble dynamics formation	[77]

Table 7 Numerical and experimental analysis on the effect of Al_2O_3 and water base nanofluid in a circular microchannel

S.no	Study type	Reynolds number	Particle size/nm	Particle Conc./%	Max. H.T gain	Outcomes	Ref
1	Numerical	–	1–100	1–4	–	Nu variation diminishes along the flow direction	[78]
2		500–1900	38	1–4	–	Nanofluids temperature-dependent characteristics boost heat transfer while decreasing entropy, shear stress, and pressure loss	[79]
3		15–100	13–47	1–5	–	The thermal properties would be better when nanofluid is utilized as the working fluid	[80]
4		< 250	29–47	0–4	–	The use of nanofluid has a major effect on pumping power, which rises with particle volume fraction and Re	[81]
5		0–58	36	0–2	–	Maximum thermal enhancement factor for symmetric ribs is 2.2517	[82]
6		2.7–87	36	9–13	–	The temperature-dependent fluid characteristics may have a substantial impact on the best outcomes	[83]
7		5–11,980	23	0–5	83	Laminar nanofluid flow enhances heat transfer more than turbulent nanofluid flow does	[84]
8	Experimental	200–1000	36	0–2	–	Nanoparticles cause catastrophic failure in two-phase cooling by depositing in massive clusters at the channel outlet	[85]
9		–	–	0–0.77	10.6	The Nu of nanofluids is higher than that of deionized water, and it increases with the growth of Re and particle concentration	[86]

power, the nanofluids enhanced the thermal performance of the microchannel.

Yang et al. [42] investigated a trapezoidal MCHS utilizing a CuO–water nanofluid as the cooling fluid. The results indicated that the two-phase model was more accurate than the single-phase model.

Duangthongsuk and Wongwises [43] conducted an experimental investigation of the heat transfer and pressure

drop in a zigzag MCHS. The study found that there was a 2–6% improvement in heat transfer performance between the cross-cutting zigzag heat sink (CCZ-HS) and continuous zigzag heat sink (CZ-HS). Additionally, the particle concentration had a significant impact on the heat transfer, but it did not affect the pressure drop.

Martinez et al. [44] investigated the thermal characterization and stability of water–ZnO nanofluids in a rectangular

Table 8 Numerical, experimental, and analytical analysis on the effect of Al₂O₃ and water base nanofluid in a parallel plate MCHS & MCHE

S.no.	Study type	Reynolds number	Particle size/nm	Particle Conc./%	Max. H.T gain	Outcomes	Ref.
1	Numerical	–	20	2–6	–	Nanomaterials facilitate the flow of fluid toward the wall as heat flux increases, thereby enhancing heat transfer	[87]
2		0.5–2	–	0–0.2	–	Entropy production reduces as the nanomaterial volume % and suction Re increases, whereas the Grashof number, radiation parameter & conduction–radiation factor decreases	[88]
3		5–50	36	0–4	–	Recirculation zones generated behind the baffles are the major mechanism for improved heat transfer	[89]
4		< 16	47	0–4	21	The enhanced thermal conductivity of nanoparticles leads to a higher flow of energy through the fluid	[90]
5	Analytical	< 1	25	0–2	–	Heat transfer is reduced when the volume % of nanoparticles increases	[91]
6		–	1–10	0.02–0.1	–	Smaller nanoparticles work better in magnetic fields than bigger ones	[92]
7		150	5	0–4	–	Under symmetric heating, nanofluids show the highest increase in heat transfer coefficient, with an average enhancement of 47%, compared to asymmetric heating	[93]
8		< 2300	60.4	0–8	–	In the laminar regime considering the effect of viscous dissipation, the heat transfer coefficient significantly decreases with increase in nanoparticle volume percentage	[94]
9		–	20	2–10	–	A strong magnetic field and high slip velocity at the walls have a negative impact on the thermal performance of nanomaterials	[95]
10		–	1–10	2–10	–	The thermophysical parameters of nanofluids have little effect on their flow fields and heat transfer behavior	[96]
11		–	–	0–8	–	The heat transfer performance improves with an increase in the volume fraction of nanomaterials	[97]
12	Experimental	–	–	0.001	–	With increase in mass flow and initial subcooling, critical heat flux rises	[98]

MCHS with Re ranging from 200 to 1200. The numerical findings revealed that using nanofluids promotes heat transfer at low Re, with the greatest increase in heat transfer coefficient (42.33%). At a concentration of 1 mass%, there was also a decrease in the base temperature of the microchannel, which was more noticeable at a low Re.

In addition, several researchers have conducted comparative investigations on various metallic oxide nanoparticles employed in microchannels. Mohammed et al. [45] investigated the influence of Al₂O₃, Ag, CuO, diamond, SiO₂, and TiO₂ nanofluids on the cooling performance of triangular MCHS. They found that the addition of nanoparticles to the coolant resulted in a decrease in the thermal resistance of the triangular MCHS, with diamond-H₂O nanofluid showing the greatest improvement at a nanoparticle concentration of 1%.

Salman et al. [46] numerically analyzed the thermal performance of microtubes. Various types of nanofluids, including Al₂O₃, CuO, SiO₂, and ZnO, were utilized in the study. The nanoparticles had sizes of 25, 45, 65, and 80 nm, and the volume fractions ranged from 1 to 4%. Ethylene glycol was chosen as the base fluid for the nanofluids. According to their findings, the SiO₂-ethylene glycol nanofluid had the highest Nu. The Nu increased with the volume fraction in all circumstances but decreased as the diameter of the nanoparticles increased.

Table 6 displays a comparison of numerical, experimental, and analytical analyses investigating the impact of Al₂O₃ and water-based nanofluids on rectangular microchannels. Based on the table's results and study type, it can be inferred that more than half of the research on Al₂O₃ nanomaterial

Table 9 Numerical and experimental investigation of the effect of CuO nanofluid in a rectangular microchannel

S.no.	Study type	Reynolds number	Particle size/nm	Particle Conc./%	Max. H.T gain	Outcomes	Ref.
1	Numerical	1–100	10	0–5	100	In laminar forced convection, for Reynolds numbers below 10, the influence of Brownian force on flow and heat transfer properties is significant	[99]
2		100–1000	30	1–6	–	A novel correlation has been introduced to compute the Nu as a function of Re, Prandtl number, and blockage ratio	[100]
3		50	10	0.4	–	Nanofluid enhances heat transfer in both porous media and fin approaches	[101]
4		10,000–60,000	100	0–4	–	Using semi-attached rib in microchannel produces greater vortices, resulting in enhanced fluid layer mixing	[102]
5	Experimental	–	20–80	0.2–0.4	–	Elevating the bulk temperature of nanofluids helps to prevent the aggregation of particles into larger clusters	[103]
6		< 1800	40	0–0.2	40	At a Re of 1150, the heat transfer coefficient of nanofluid with a volume fraction of 0.2 exhibited an increase of approximately 40% compared to deionized water	[104]
7		< 5000	29	0–4.5	–	At a specific Re, the energy efficiency of nanofluids, as determined by the ratio of heat transfer to pumping power, is still lower than that of water	[105]

Table 10 Effect of TiO₂ based nanofluid in a rectangular cross section microchannel

S.no.	Study type	Reynolds number	Particle size/nm	Particle Conc./%	Max. H.T gain	Outcomes	Ref.
1	Numerical	–	–	0.01–0.9	–	Nanofluids are an excellent choice for designs that need lower volume flow rates and have lower nanoparticle volume fractions	[106]
2		100–250	21–60	1–2.3	–	Approximately 14% is the highest normalized efficiency of the longitudinal vortex generator microchannel in comparison with the plain channel. In addition, the use of nanofluid may boost the normalized efficiency by 27%	[107]
3		200–1200	6	1–3	19.66	At low Re, the findings indicate that the use of nanofluids and the lowering of microchannel height boost heat transfer	[108]
4	Experimental	50–850	25	0.25–2	–	In comparison with pure water, TiO ₂ particles in the base fluid produced greater heat transfer and did not create an excessive rise in pressure drop	[109]
5		100–750	25	0–2	39.7	The heat resistance of the base fluid is reduced by introducing particles with an average diameter of less than 25 nm	[110]
6		250–1700	–	0–2	–	Using the Maxwell model to measure thermal conductivity provides an accurate estimation of the Nu	[111]
7		–	15	0–0.1	–	Nanofluids have distinct droplet-forming features based on temperature	[112]

Table 11 Investigation on the effect of various nanofluids on the thermal performance of various MCHS and MCHE geometry

S.no.	Study type	Geometry	Reynolds number	Nanoparticle	Particle size/nm	Particle Conc./%	Max. H.T gain	Outcomes	Ref.
1	Experimental	Semicircle, trapezoidal, square	250–850	Al ₂ O ₃	40–50	0–0.25	4.6	The Nusselt number (8.54% & 26.4%) and heat transfer rate (3.13% & 5.87%) are higher in the trapezoidal channel compared to the square and semicircular channels	[113]
2		Trapezoidal	190–1020	Al ₂ O ₃	56	0–0.26	15.8	Replacing water with nanofluids reduces thermal resistance of the MCHS at almost constant pumping power	[114]
3		Cylindrical	<900	CuO	25	0.05–0.3	23	Pure water has lower Nu compared to nanofluids with 0.05 mass%, 0.1 mass%, and 0.3 mass% concentration, with percentage increases in Nu being 17%, 19%, and 23%, respectively	[115]
4			<900	Cu	25	0.05–0.3	–	The thermal resistances decreased by up to 21% when the mass fraction of particles increased from 0.05 to 0.3 mass%	[116]
5		Circular	500–4000	Al ₂ O ₃ TiO ₂ SiO ₂	13 10–25 18	0–1	15.3	Al ₂ O ₃ nanofluid with a 1% volume concentration was found to have the greatest thermal performance	[117]
6		Rectangular	–	SiO ₂	35–190	1.4–7	–	The increase in viscosity of nanofluids can be explained using a conventional model, but with a modification based on the particle size, which affects the crowding factor	[118]
7			100–350	Al ₂ O ₃ SnO ₂	–	0–5 0–1	13 14	The findings suggest that using 5% Al ₂ O ₃ and 1% SnO ₂ nanofluids in MCHS resulted in a heat transfer improvement of 13% and 14%, respectively, compared to the base fluid	[119]
8			<100	CuO SiO ₂	43	0.1–0.25	32.8	Al ₂ O ₃ –water nanofluid outperforms SiO ₂ –water nanofluid in heat transfer due to its higher thermal conductivity	[120]
9			–	Bi ₂ O ₃ Fe ₃ O ₄ TiO ₂ SiO ₂	200–300 90–210 50–100 <100	–	–	There exists a specific concentration limit for all nanofluids, beyond which increasing the concentration does not lead to any further reduction in pressure drop or system drag	[121]
10			200–500	Al ₂ O ₃ TiO ₂	5 5	0–1	42.9	The thermal conductivity and dynamic viscosity of Al ₂ O ₃ and TiO ₂ nanofluids are positively affected by an increase in particle volume fraction	[122]
11	Numerical	Trapezoidal	<1200	CuO	100	1–4	–	Taking viscous dissipation into account, it is shown that pressure drop fluctuates relatively slow	[123]
12			100–900	Al ₂ O ₃ TiO ₂	5 5	0.1–1	36.6	When compared to a MCHS made of stainless steel at Re = 900, using copper instead can increase the total thermal resistance by up to 76%	[124]
13		Helical	–	Al ₂ O ₃	–	–	–	Helical-shaped geometry can greatly enhance convective heat transfer, and reducing the helix radius can further improve the thermal performance	[125]

Table 11 (continued)

S.no.	Study type	Geometry	Reynolds number	Nanoparticle	Particle size/nm	Particle Conc./%	Max. H.T gain	Outcomes	Ref.
14		Converging	100–600	TiO ₂	10	0–0.5	90	Raising the convergence angle and reducing the aspect ratio of the channel increases the flow velocity within the channel	[126]
15		Rectangular	< 100	SiO ₂	–	0–1	–	Almost the same amount of pressure is lost by all particles distributed in water; however, heat transfer is greatest for H ₂ O–diamond nanofluids and least for H ₂ O–SiO ₂ nanofluids	[127]
16			140–1400	Fe ₃ O ₄	13	0–0.8	–	When fluid enters the channel entrance, the Nu is at its greatest	[128]
17			140–1400		–	0.4–0.8	–	As the volume fraction increases, the thermal conductivity also increases and heat capacity decreases, resulting in a temperature drop	[129]
18			100–500		30	0–4	–	The application of a non-uniform magnetic field initially reduces the entropy production due to heat transfer, but it subsequently increases	[130]
19			–	SiC, TiO ₂	–	1–9	–	For the same volume fraction, TiO ₂ nanofluid has a lower thermal resistance than SiC	[131]
20	Analytical	Rectangular	3000	Al ₂ O ₃ SiC	20	0–4	–	SiC–water nanofluid reduces cell temperature more effectively than Al ₂ O ₃ –water nanofluid	[132]

for nanofluid production is based on numerical analysis. The table also indicates that the use of smaller diameter nanoparticles and increasing the volume percentage of nanoparticles enhances heat transfer. Moreover, higher heat transfer coefficients are observed in flow regimes with higher Re .

(c) Hybrid nanofluids used in various microchannel geometries

Hybrid nanofluids are advanced nanofluids that are created by mixing two distinct nanoparticles in a base fluid. Preparation method of hybrid nanofluid is shown in Fig. 10. Hybrid nanofluids have superior thermal characteristics compared with base fluids and nanofluids. These fluids exhibit better characteristics than ordinary fluids, such as

- Offer superior thermophysical properties in comparison with mono-nanofluids.
- High dispersion stability and Brownian motion of particles.
- A remarkable increase in thermal conductivity with varying particle concentrations.
- Reduction in pumping power compared with conventional fluid power.
- High surface area and high heat transfer between fluid and particles.
- Increased control over thermodynamic and transport properties.

Turcu et al. [133] were the first to use polypyrrole–carbon nanotubes (CNTs) and multiwall carbon nanotubes (MWCNTs) on magnetic Fe_3O_4 hybrid nanoparticles to create hybrid nanofluids. Jha et al. [134] combined silver nanoparticles with multiwall carbon nanotubes (MWCNTs) to create hybrid nanofluids. The results show the improved

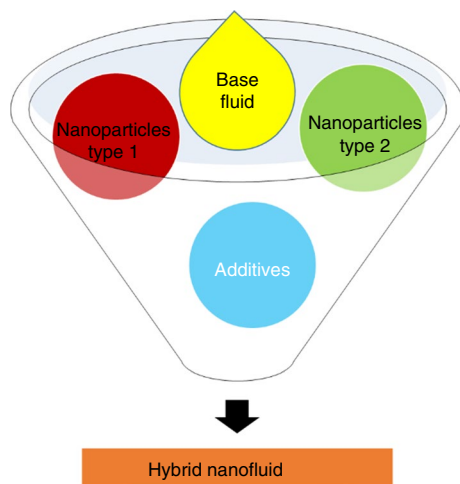


Fig. 10 Preparation of hybrid nanofluid

thermal properties of the hybrid nanofluids. Suresh et al. [135] created hybrid nanofluids by mixing Al_2O_3 and Cu and found that there was an enhancement in thermal conductivity of 12.11% with a volume concentration of 2%. To improve the thermal performance of MCHE, an experimental investigation was conducted by Yushuang Huang et al. [136]. They incorporate β -cyclodextrin- ZrO_2 as a nanoparticles and ethylene glycol as the base fluid for construction of nanofluids. They found that fabrication of nanofluids utilizing β -cyclodextrin-modified ZrO_2 nanoparticles holds significant potential for enhancing heat transfer in microelectronic microchannels. Table 12 shows numerous studies in MCHS and MCHE that use hybrid nanofluids as their working fluid. Table 12 shows that nearly 50% of hybrid nanofluid research relies on numerical analysis. The most commonly used nanomaterials for creating hybrid nanofluids are alumina and copper oxide. Additionally, rectangular cross sections are frequently utilized for constructing microchannels in comparison with other geometries. Based on the outcomes of the above literature survey, it can be concluded that increasing particle concentration and Re leads to improved heat transfer in the microchannel, although this may also result in higher pumping power requirements. Mansouri et al. [137] conducted an experiment to assess the convective heat transfer of a hybrid nanofluid consisting of graphene oxide and gold in a CPU. They varied the concentrations of graphene oxide and gold (ranging from 0.0044 to 0.0114% by mass) as well as the Reynolds number (ranging from 676 to 2185) to optimize the overall performance of the device. The experimental findings indicated that the nanofluid composed of graphene oxide and water, decreased the CPU's surface temperature by 10.6% and 16.2%, respectively, compared to using DI water alone.

Srivastava and Sahoo [138] conducted an experiment to examine the impact of nanoparticles with different shapes on the thermo–hydro performance of a microchannel heat sink (MCHS). The experiment utilized water as the reference fluid. The results showed that the hybrid nanofluid composed of dissimilar-shaped nanoparticles demonstrated improved performance in terms of heat transfer coefficient, Nusselt number, as well as inlet and outlet exergy.

(d) Nanofluids used in various microchannel geometries suspended with carbon nanoparticles

Studies have investigated the cooling performance of MCHS using carbon nanotubes (CNT). Ebrahimi et al. [155] investigated the cooling performance of an MCHS using carbon nanotubes (CNT). It is found that increasing the nanolayer thickness of multiwalled carbon nanotubes (MWCNTs) decreased the MCHS temperature gradient.

Arabpour et al. [156] performed a numerical simulation of an MCHS using kerosene nanofluid/MWCNTs and found

Table 12 Hybrid nanofluids used in various microchannel geometries

S.no	Study type	Geometry	Reynolds Number	Nanoparticle	Particle size/nm	Particle Conc./%	Max. H.T gain	Outcomes	Ref
1	Numerical	Trapezoidal	300–1100	Al ₂ O ₃ , CuO	20–60	0–8	–	The findings demonstrate that when particles are 34 nm in size, the average Nu rises fast; however, when particles are 60 nm in size or larger, heat transfer is not significantly affected	[139]
2		Rectangular	200–600	Al ₂ O ₃ , CuO	43 29	0–4	–	For higher and lower Re, the pumping power and performance index are not affected by volume fraction	[140]
3			100–800		30	1–4	39	Higher heat transfer improvement may be seen by increasing the volume percentage of nanoparticles	[141]
4			100–900		29–36	0–5.3	53.06	Irreversibility in the MCHS with longitudinal vortex generator might be decreased by employing nanofluids as the working fluid	[142]
5			–		35–50	0–4	–	Cu–water nanofluid is a better thermal conductor than Al ₂ O ₃ –water nanofluid	[143]
6			–		–	1–5	–	When flow rates are large, the volume flow rate dominates heat transfer, and nanomaterials have little effect on the heat absorption	[144]
7			–	Cu, Diamond	6 2	0–1	–	Using water–diamond nanofluid in a MCHS at a fixed pumping power of 2.25 W can improve its cooling performance by around 10% compared to pure water	[145]
8		Trapezoidal grooved	266–798	Al ₂ O ₃ , CuO, ZnO, SiO ₂	25	0–4	–	In grooved MCHS, secondary flow increases both the hydrodynamic & thermal boundary layer disturbances, resulting in higher heat transfer	[146]

Table 12 (continued)

S.no	Study type	Geometry	Reynolds Number	Nanoparticle	Particle size/nm	Particle Conc./%	Max. H.T gain	Outcomes	Ref
9		Semicircle	–	CuO, Al ₂ O ₃	28.6–29 38.4–47	–	–	Enhanced heat transfer can be achieved by raising both the volume fraction of nanoparticles and Re	[147]
10		Parallel Plates	10–100	Al ₂ O ₃ , Ag	10	0–4	–	Increasing slip coefficient reduces Nusselt number (Nu), while higher Hartmann numbers lead to larger slip velocity	[148]
11	Experimental	Rectangular	200–500	Al ₂ O ₃ , TiO ₂	5 5	0–1	42.9	Using Al ₂ O ₃ nanofluids, a fan-shaped MCHS exhibits better heat transfer performance compared to a rectangular MCHS	[122]
12			–	Nano PCM	120	0–3	–	The heat transfer coefficient of a slurry containing 30% bare indium nanoparticles can achieve up to 47,000 W m ⁻² K ⁻¹ when the flow rate is 3.5 mL s ⁻¹	[149]
13			500– 2000	Al ₂ O ₃ , CuO	20 40	0–1	49 27	CuO nanoparticles in a water-based fluid are more prone to deposition than Al ₂ O ₃ , but they exhibit superior heat transfer performance.	[150]
14		Serpentine	100– 1500	CuO, Al ₂ O ₃	15	0–0.3	–	Compared to Al ₂ O ₃ -H ₂ O and base fluids, CuO-H ₂ O nanofluid has a higher heat transfer coefficient	[151]
15	Analytical	Rectangular	–	Al ₂ O ₃ , CuO	25–45	0–4	–	An increase in nanoparticle volume fraction enhances Brownian motion, which significantly affects the heat transfer process by dissipating heat to the surroundings	[152]
16			–	Cu, Al ₂ O ₃ , Ag, TiO ₂	25–45	0–8	–	Increasing the volume % of nanoparticles enhances Brownian motion, reducing the temperature difference between the coolant and the wall	[153]

Table 12 (continued)

S.no	Study type	Geometry	Reynolds Number	Nanoparticle	Particle size/nm	Particle Conc./%	Max. H.T gain	Outcomes	Ref
17		Circular	10,000	Al ₂ O ₃ , Cu	–	2–6	–	Compared to the larger nanoparticles, smaller nanoparticles generated less entropy in nanofluids of all concentration	[154]

that Nu was strongly influenced by the application of an oscillating heat flux at Re values of 10 and 100.

Studying the impacts of porous media on fluid flow and heat transfer in a microchannel filled with MWCNT/Oil Nanofluid. Nojoomizadeh and Karimipour [157] studied the impacts of porous media on fluid flow and heat transfer in a microchannel filled with MWCNT/oil nanofluid and found that a higher Re resulted in a decrease in the heat transfer time between the nanofluids and walls, resulting in a higher local Nusselt number. Table 13 lists various carbonaceous nanofluids used in MCHE and MCHS.

Table 13 indicates that over 50% of research on carbon nanomaterial suspended nanofluids relies on numerical analysis. Rectangular cross sections are also commonly used in constructing microchannels, as noted in the table. According to the literature survey, the use of carbon nanoparticles in nanofluid creation leads to a decrease in thermal radiation and improved thermal performance at high temperatures. Furthermore, the enhancement in heat transfer is more prominent at higher Re.

Flow disruption in MCHS

To enhance heat transfer performance, flow disruption is an effective approach that increases mixing and heat transfer by inducing flow instabilities. Turbulent flow is a prevalent method for flow disruption, but in many cases, low velocities or small hydraulic diameters prevent the flow from reaching the crucial Reynolds number. To overcome this, efforts are being made to introduce geometrical alterations to the channel sidewalls, such as grooves, ribbed channels, wavy channels, dimples, and fins, which act as periodic disturbance promoters. These promoters induce self-sustaining oscillations, leading to flow instability and improved mixing. Many studies have investigated the use of different disturbance promoters to enhance flow mixing in conventional channels.

Flow disruption in MCHS introduces various types of wavy channels

Rectangular straight channels are a common choice for MCHS due to their low pumping power and laminar flow

resulting in almost straight streamlines. However, these channels have several disadvantages. Firstly, the heat transport is poor due to insufficient fluid mixing caused by the linear streamlines. Secondly, the flow and heat transfer boundary layers thicken throughout the flow path because of the single-direction flow characteristics, leading to a larger temperature difference across the channels, especially at high heat fluxes. Thirdly, these channels are not effective in removing local high heat fluxes in microelectronic devices with hot spots. To overcome these challenges, several theoretical, experimental, and computational methods have been used to enhance the flow and heat transfer performance of MCHS by introducing different channel designs, such as grooves, ribbed channels, wavy channels, dimples, and fins, that promote flow instability and mixing.

When a fluid flows through a curved channel, it experiences not only primary motion but also a secondary motion in the plane of the cross section, which is referred to as the Dean vortex. The Dean vortices arise from centrifugal forces that act on the fluid as it flows through the curved channel. The presence of these vortices induces flow components to stretch and fold, which enhances the fluid mixing and heat transfer. The Dean vortices have been shown to be particularly effective at promoting mixing and heat transfer in microchannels, where the low Reynolds numbers limit the potential for turbulent flow. Consequently, many researchers have investigated the use of curved channels or modified channel geometries that induce Dean vortices as a means of improving the flow and heat transfer performance of microchannels. Sui et al. [165] proposed a new design for an MCHS, which was influenced by Dean vortices. Instead of using straight channels, they suggested using wavy channels that showed superior heat transfer performance when compared to straight microchannels of equivalent cross section. However, the use of wavy channels resulted in a pressure drop penalty, which could be offset by enhancing the heat transfer capability.

In addition, Sui et al. [166] performed experiments to compare the performance of MCHS with wavy channels and those with straight channels. They calculated both the overall Nusselt number and the friction factor to confirm the superior performance of the wavy design. Wavy MCHS with rectangular cross sections and amplitudes ranging from

Table 13 Nanofluids used in various MCHS & MCHE suspended with carbon nanoparticles

S.no.	Study type	Geometry	Reynolds number	Particle size/nm	Particle conc./%	Max. H.T	Outcomes	Ref.
1	Numerical	Helical	1–100	30	0–0.25	–	The increase in Nu is more significant at higher Re when the slip coefficient and mass percentage of nanoparticles are increased	[158]
2		Rectangular	–	25	0–1	–	Increasing nanolayer thickness in MCHS enhances thermal conductivity and reduces the temperature gradient	[155]
3			10–100	–	–	–	Addressing thermal radiation in the near-field media can lead to further improvement in heat transfer in microchannels using nanofluids	[159]
4			10–100	–	0–8	–	Using oscillating heat flux has a substantial impact on the profile figure of the Nu in various Reynolds numbers	[156]
5			150–700	–	0–8	–	As Re and nanoparticle volume fraction increase, heat transfer increases and thermal resistance decreases	[160]
6			0.1–10	30	0–0.4	–	The rise in the local Nu would be higher, for higher Re, low porosity and Darcy	[157]
7			–	9.2 nm 1.5 μ m	0–0.1	13	Thermal resistance is reduced by 3% at 40 °C when CNT nanofluid is used in place of water	[161]
8		Parallel Plates	0–100 1592–478	–	0–0.25	30	It is noted that a lower Darcy Number results in a greater local Nu and porous medium causes higher slip velocity	[162]
9	Analytical	Rectangular	–	9–10 nm 15 μ m	–	13	Nanofluids as working fluids decrease overall thermal resistance and improve the thermal performance at high temperatures	[163]
10	Experimental		100–1400	–	0.01–0.1 mass	29	Increasing flow rate and mass concentration enhances heat transfer coefficient in MCHS, while higher heat fluxes have minor impact	[164]

125 to 500 m were investigated numerically by Mohammed et al. [167]. According to their findings, the friction factor and wall shear stress increased in direct proportion to microchannel amplitude.

Liquid-cooling parallel-flow and counter-flow double-layer wavy MCHS with Re of 50–110 were studied by Xie et al. [168]. The findings show that the counter-flow double-layer wavy MCHS operates better at higher flow rates and provides a more consistent temperature rise. Using nanofluids as coolants, Sakanova et al. [169] investigated for the first time how the wavy walls of an MCHS promote heat transfer. The findings revealed that the wavy MCHS outperformed a

regular rectangular MCHS. There is a 5.34–24.1% increase in heat transfer and a pressure drop of around 150–421.7%. Chiam et al. [170] conducted a numerical investigation to study fluid flow in microchannels with secondary branches in the Re range of 50–200. The numerical results show that the heat transfer performance of the system can be improved by adding extra branches. Pandey et al. [171] conducted a numerical analysis to assess the performance of a straight MCHE with wavy channels. Their findings indicate that wavy channels outperform straight channels in terms of thermal performance. On the other hand, when considering pumping power, straight channels exhibit better

characteristics. Table 14 represent various studies on wavy channels, along with the most important conclusions from each.

Flow disruption in microchannels by introducing various types of ribs

Several experimental and computational studies have been carried out to assess the impact of ribs on the thermohydraulic efficiency of MCHS & MCHE. Ribs are implemented to enhance heat transfer by disrupting the thermal

and hydraulic boundary layers. These ribs are frequently referred to as turbulators or roughness components, respectively. Ribs can also promote flow mixing by producing vortices and causing chaos during advection. However, the heat transfer boost provided by the ribs was accompanied by a large pressure loss penalty. Consequently, optimizing the ribs was necessary to ensure a lower pressure drop. Table 15 presents the impact of ribs on the hydrothermal performance of MCHS and MCHE.

In an experimental and numerical analyses, Wang et al. [177] examined the heat transfer performance of an MCHS

Table 14 Investigation of wavy channels used in microchannels

S.no.	Wavy pattern type	Shape of microchannel	Reynold number	Outcomes	Ref.
1	Left-right		100–600	The utilization of a curved path increases the transfer of heat and the resistance to flow by 53% and 154% correspondingly	[165]
2	Wavy channel with a rectangular cross section		300–800	The transfer of heat and loss of pressure were both elevated by 49% and 111%, respectively	[166]
3	Left-right		100–1000	Wavy microchannels exhibit better heat transfer performance than straight microchannels of equal cross-sectional area	[167]
4	periodic, wavy shape with rectangular channel		65–333	Liquid flowing through bends produces Dean vortices, or symmetric secondary flow, as a consequence of steady flow	[172]
5	Double-Layer Wavy MCHS		50–110	The double-layer counter-flow wavy MCHS performs better at higher flow rates and the temperature rise is more consistent	[168]
6	Longitudinal & transversal-wavy MCHS		50–320	Increase in heat transfer between 6.1% to 27.3% and a decrease in pressure between 123.3% to 149.2% is found	[173]
7	Wavy channels with alternate secondary branches		50–200	Introducing secondary branches has the potential to increase performance	[170]
8	Up-down		10–100	In comparison with microchannels with straight walls, wavy channels enhance overall performance by up to 26%	[174]
9	Up-down		50–150	Compared to channels with straight walls, a 55% improvement in total performance	[164]
10	Up-down		100–240	Wavy channel has a positive influence because it reduces the thermal and hydrodynamic boundary layer	[176]

with bidirectional ribs (BR) at Reynolds numbers from 100 to 1000. Their findings indicated that the Nusselt number (Nu) of the BR microchannel could reach up to 1.42 times higher than that of a microchannel featuring vertical or spanwise ribs.

Interrupted MCHS in transverse microchambers with various rib forms have been studied by Chai et al. [178]. The transverse microchambers in the interrupted MCHS exhibit a decrease in thermal resistance of 4–31% and a reduction in entropy production rates of 4–26% compared to those of the straight MCHS.

With fan-shaped ribs on the sidewalls, Chai et al. [179] numerically investigated the thermal and hydraulic parameters of laminar flow in an MCHS. The findings indicated that the heat transfer properties were significantly influenced by the height and spacing of the fan-shaped ribs, while the width of the ribs had a lesser impact.

Desrues et al. [180] examined heat transfer and pressure loss in 3D channels featuring alternating opposing ribs. The study found that while the pressure drops increased consistently with Re, heat transfer only improved after Re exceeded a critical value.

Chai et al. [181] utilized numerical simulations to evaluate the thermohydraulic performance of an MCHS that incorporated triangular ribs on the sidewalls. The implementation of these ribs successfully restricted the temperature increase of the heat sink base and prevented a decrease in the local heat transfer coefficient in the flow direction.

The effects of rib shape and fillet radius on the thermal-hydrodynamic performance of an MCHS were investigated numerically by Derakhshanpour et al. [182]. The study revealed that increasing the rib corner curvature resulted in a higher heat transfer coefficient, but also led to an increase in the pressure drop. Using a water–TiO₂ nanofluid, Gravndyan et al. [183] conducted investigation on the thermal performance of a rectangular MCHS and studied the impact of rib aspect ratio. The study found that the friction factor was independent of the rib aspect ratio, but dependent on the volume percentage of nanoparticles in the nanofluid.

The use of ribs in microchannels can cause significant pressure loss due to high-flow disruptions, so the optimization of rib geometry is necessary. In order to improve heat transfer while maintaining a minimum pressure drop, grooves or cavities are used to restrict flow and redevelop the thermal boundary layer. Cavities can enhance heat transfer by encouraging mixing between fluid layers near the wall and core through the action of jets and flow throttling. The idea of the ribs and cavities working together has also been used as an effective way to improve heat transfer. Ghani et al. [184] investigated the thermohydraulic characteristics of a microchannel with both sinusoidal cavities and rectangular ribs (MC-SCRR). The results showed that MC-SCRR performed better in terms of thermal performance compared to

both rectangular microchannel ribs and sinusoidal microchannel cavities alone. This suggests that the combination of ribs and cavities is an effective way to enhance heat transfer. Xia et al. [185] conducted a numerical analysis to investigate thermal enhancement in an MCHS by using fan-shaped reentrant cavities & internal ribs. They found that the Nu for the fan-shaped reentrant cavities was 1.3–3 times higher than that for a rectangular microchannel. The heat transfer characteristics of an MCHS with triangular cavities and rectangular ribs were numerically studied by Li et al. [186]. Their findings revealed a significant improvement in heat transfer for microchannels equipped with triangular and rectangular cavities.

On the other hand, the combination of ribs and grooves was found to be effective way in enhancing heat transfer and reducing pressure drop. This is due to the high-flow disruption capability of ribs and the lower pressure drop of grooves. To validate this Zhu et al. [187] investigated the thermal and hydraulic performance of an MCHS with rectangular grooves and ribs and found that the combination of grooves and ribs was effective in enhancing heat transfer and reducing pressure drop due to the high-flow disruption capability of ribs and the lower pressure drop of grooves. They concluded that the combination of grooves and ribs can significantly increase the overall performance. Further, the thermal performance of an MCHS with ribs and grooves was experimentally and numerically investigated by Wang et al. [188] for chip cooling applications. Their findings showed that rib-grooved microchannels had a Nu 1.11–1.55 times higher than smooth microchannels.

In addition, the use of porous media is a viable solution to mitigate the high pressure drop associated with the implementation of ribs in MCHS. Porous media are frequently employed in heat transfer applications due to their large surface area that comes in contact with the fluid, which enhances the heat transfer performance. The thermohydraulic characteristics of microchannels with solid and porous ribs have been numerically examined by Li et al. [189]. They found that the thermal performance of microchannels with ribs was better than that without ribs. However, the pressure drops and friction factors were higher for microchannels with solid ribs compared to those with porous ribs. By replacing solid ribs with porous ones in center, symmetrical, and staggered rib arrangements, the pressure drops were reduced by 67%, 57%, and 12%, respectively. Wang et al. [190] conducted a numerical investigation to examine how the combined use of porous/solid fins and nanoparticles affects the cooling efficiency of microchannel heat sinks (MCHS). The results showed that, under constant Reynolds number conditions, heat sinks composed of metallic foam exhibited superior cooling performance. These heat sinks were capable of significantly reducing the surface temperature of the heat sink compared to other configurations. In

Table 15 Flow disturbance of MCHS & MCHE using ribs

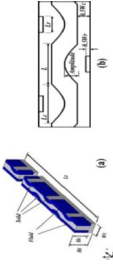
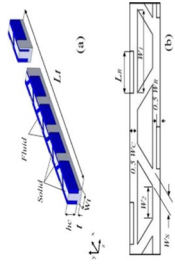
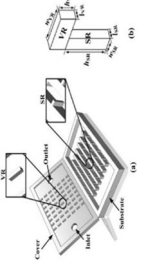
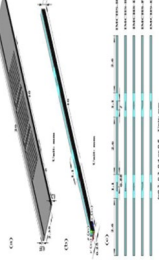
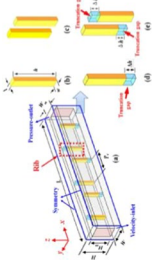
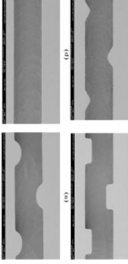
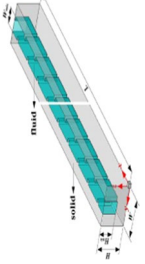
S.no.	Geometry	Shape	Re. No.	Outcomes	Ref.
1	MCHS with sinusoidal cavities & rectangular ribs SCRR		100–800	MCHS with SCRR outperforms both MCHS rectangular ribs and MCHS with sinusoidal cavities in terms of thermal performance	[184]
2	MCHS with secondary oblique channels in alternate directions & rectangular ribs (SOCRR)		100–500	MC-SOCRR outperformed both MC-RR and MC-SOC in terms of overall performance	[194]
3	MCHS with bidirectional ribs (BR)		100–1000	Nu of the BR microchannel is up to 1.4–2 & 1.2–1.42 times higher than vertical ribs microchannels & spanwise rib microchannel, respectively	[177]
4	Interrupted MCHS (IMCHS) with ribs		187–715	In comparison to a straight MCHS, IMCHS with ribs in the transverse microchannels exhibit a 4–31% drop in thermal resistance and 4–26% drop in entropy production	[178]
5	MCHS with truncated rib on the sidewall		100–1000	Truncated rib may improve the thermal performance by minimizing the pressure drop penalty while maintaining heat transfer	[195]
6	Rectangular, triangular, and semicircular ribs		1000	Micro-ribs can improve the heat transfer rate of microchannels but they also increase the pressure drop penalty	[196]
7	MCHS with offset ribs on sidewalls		(190 ≤ Re ≤ 838)	Offset ribs lead to a considerable improvement in heat transfer but also result in a higher pressure drop	[197]

Table 15 (continued)

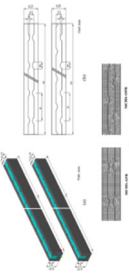
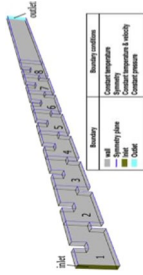
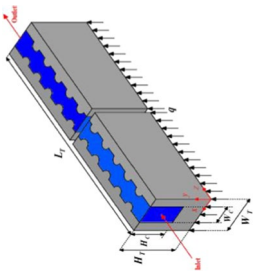
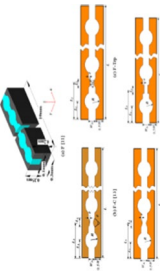
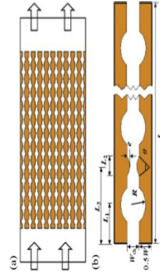
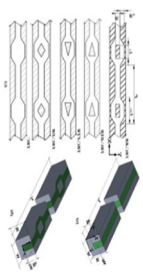
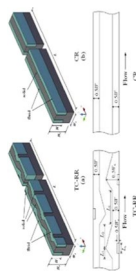
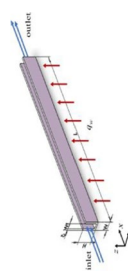
S.no.	Geometry	Shape	Re. No.	Outcomes	Ref.
8	MCHS with fan-shaped ribs on sidewalls		187–715	Height and spacing of fan-shaped ribs have a big influence on heat transfer capabilities, whereas rib width has less impact	[179]
9	Rectangular duct with streamwise-periodic transverse rectangular ribs		75–2000	Pressure drop increases monotonically with Re, but heat transfer is improved only when Re exceeds a threshold value	[180]
10	Semicircular ribs (MC-SCR), semi-elliptic ribs (MC-SER), semicircular ribs with filleted corner (MC-SCR-FR) and semi-elliptic ribs and filleted corner (MC-SER-FR)		198	Microchannel with semicircular ribs and MC-SER heat sinks, the two designs of MC-SCR-FR and MC-SER-FR increase the Nusselt No. by 18–21% and 0.5–10%, respectively	[198]
11	fan-shaped reentrant cavities with various ribs		> 300	When the Re exceeds 300, the combination of fan-shaped reentrant cavities and trapezoidal ribs appears to be the most viable option, while the use of circular ribs in fan-shaped reentrant cavities provides the best results	[199]
12	MCHS with fan-shaped reentrant cavities and internal ribs		150–600	Nu for fan-shaped reentrant cavities is between 1.3 & 3 times that of rectangular MCHS	[185]
13	Rectangular channel with trapezoidal cavities and four different ribs		140–600	Diamond rib combination had the best thermal performance and the backward triangular rib combination had the largest entropy production	[200]

Table 15 (continued)

S.no.	Geometry	Shape	Re. No.	Outcomes	Ref.
14	MCHS with triangular cavities and rectangular ribs		500	A microchannel with triangular cavities and rectangular ribs shows a significant improvement in heat transfer compared to a smooth microchannel	[186]
15	Microchannels with solid and porous ribs		100	MCHS with ribs, whether solid or porous, has better thermal performance compared to microchannels without ribs	[189]

another research to improve the hydrothermal property of MCHS, an investigation was conducted by Li et al. [191]. They incorporate embedded module ribs and pin with fins. Their outcomes indicate that at a Reynolds number of 458, the heat transfer efficiency increased by 63.91%, resulting in a 67.65% enhancement in temperature uniformity. Furthermore, the pressure drops experienced a modest rise of merely 10.24%.

Polat et al. [192] conducted a numerical investigation to examine the heat transfer performance of a microchannel heat sink (MCHS) equipped with micro pin-fins, focusing on steady laminar flow conditions. Using ANSYS Fluent, simulations were carried out to analyze the heat and fluid flow within MCHSs featuring circular, square, and diamond-shaped micro pin-fins of equal hydraulic diameter. The arrangement of micro pin-fins in each MCHS configuration was optimized for performance using a multi-objective genetic algorithm known as Non-dominated Sorting Genetic Algorithm (NSGA-II). The results of the optimization process revealed that the square-shaped pin-fin configuration exhibited unfavorable performance compared to the other pin-fin shapes. However, among all the configurations tested, the diamond-shaped pin-fins demonstrated a significant improvement in heat transfer while maintaining an acceptable pressure drop ratio. Therefore, the diamond-shaped pin-fins were identified as the most effective choice for enhancing heat transfer within the MCHS.

Zhang and Du [193] proposed a method to enhance the heat dissipation of a MCHS by introducing fins that generate a secondary flow. In their study, they compared the performance of the finned MCHS with a straight microchannel heat sink. The experiments were conducted under a mass flow rate of 3.5 gs^{-1} . The results indicated that the finned MCHS achieved improved heat dissipation compared to the straight microchannel heat sink. Specifically, the maximum temperature of the finned MCHS was reduced by 3.04 K (equivalent to a 6.67% decrease) compared to the straight microchannel heat sink. Additionally, the average temperature of the finned MCHS was reduced by 2.86 K (equivalent to a 6.75% decrease) compared to the straight microchannel heat sink.

Channel material

The literature reviewed shows that the flow channels used in various experimental and numerical investigation were made of various materials such as aluminum (Al), copper (Cu), silicon (Si), stainless steel, & various other metals [186–188]. The use of Si is preferred in electronic devices due to its compatibility with micromachining and micro-fabrication techniques used in semiconductor manufacturing processes, making it well suited for the electronics

industry [204]. Generally, water is used as a working fluid which causes corrosion in metallic heat exchangers, owing to thermal property limitations of metallic heat exchangers, these materials become ineffective under extremely high temperatures conditions. To overcome these limitations nowadays numerous researchers have focused on ceramic microchannels.

Ceramic microchannel heat exchangers/heat sink

Metals are commonly used in heat exchangers; however, metallurgical issues or significant deformations are extremely troublesome at high heat-flux settings [190–193]. Furthermore, some fluids are corrosive, and the use of metals increases the production costs [194–197]. Ceramics are one of the finest options for high-temperature applications according to various prior studies [213, 214]. These materials exhibit excellent oxidation, sulfidation, and corrosion resistance. Ceramics generally have low thermal conductivities (e.g., zirconia [215], silicon nitride (SiC) [216]). However, a group of ceramics, such as titanium diboride (TiB₂) [217], zirconium diboride (ZrB₂), hafnium diboride (HfB₂) [218], aluminum nitride (AlN) [219], and beryllium oxide (BeO₂) [220], have better thermal conductivity.

Alm et al. [221] studied the performance in cross-flow and counter-flow regimes of an Al₂O₃ MCHE using demineralized water to measure the heat transfer rate. The efficiency varied from 0.10 to 0.22 in cross-flow heat exchangers at mass flow rates of 20–120 kg h⁻¹, while the heat transfer coefficient was 22 kW m⁻² K⁻¹. A miniaturized heat exchanger composed of SiC was experimentally investigated by Fend et al. [222] at elevated temperatures. Two SiC heat exchangers with various wall thicknesses and widths were tested and compared at temperatures up to 950 °C. The sample with a larger channel width worked better in these studies because of its lower wall thickness. Furthermore, these heat exchangers were observed to have a large heat transfer surface area to volume ratio of 995 m³ m⁻² and a high efficacy of up to 65%.

Villanueva et al. [223] explored the use of ceramics in plate heat exchangers with fins. The findings reveal that the development of vortices in the frontal area of the fins leads to an increase in the heat transfer. Lewinsohn [224] investigated a small SiC ceramic plate MCHE, reported the efficacy, temperature variations, change in pressure, and stresses developed in hot & cold fluid plates. The findings revealed that a microturbine power cycle made of ceramics may achieve greater power cycle efficiency.

Carman et al. [225] examined the impact of an MCHE composed of silicon carbon nitride (SiCN) ceramic material on a microturbine. The study suggests that design optimization can lead to an improvement in the thermal efficiency of the cycle by approximately 9%. Ponyavin et al. [226]

investigated small heat exchangers made of SiC employed for hydrogen generation. The high thermal conductivity of silicon carbide helped to eliminate temperature gradients between the channel walls and maintain low stresses, according to the results. Monteiro and de Mello [227] conducted a study on the thermal efficiency and pressure drop of plate heat exchanger with fins made of alumina. Their findings showed that increasing the mass flow rate resulted in a reduction in the pressure drop, which in turn reduced the device's efficiency. Nekahi et al. [228] studied the viability of TiB₂-SiC composites doped with a two mass% carbon fiber in an MCHE. They found that the TiB₂-SiC and TiB₂-SiC-C_f composites improved heat transfer by 15.5 percent as compared to Al₂O₃. Fattahi et al. [229] conducted a study to investigate the effect of using aluminum nitride (AlN) for constructing MCHE on its heat transfer performance. By replacing Al₂O₃ with AlN, the heat transfer and efficiency of the MCHE were improved by 59% and 26%, respectively. Vajdi et al. [230] conducted a numerical study on an MCHS made of ZrB₂ to analyze pressure drop and heat transfer. The study found that the high thermal conductivity of the ceramics resulted in an effective heat transfer rate. Table 16 summarizes numerous literature studies that use ceramic as a microchannel material.

Channel geometry

The flow in the MCHS was predominantly laminar due to the small channel size. Traditional MCHS experiences a growing thermal boundary layer which causes hotter fluids to be collected on the channel wall, while cooler fluids circulate through the core channel. Therefore, early research efforts focused on improving the thermal efficiency of a typical straight rectangular MCHS by modifying the channel length, aspect ratio, and wall thickness. While some researchers have attempted to disrupt the MCHS boundary layer, others have altered the microchannel cross section to enhance its performance, such as circular, triangular, square, and trapezoidal shapes. However, rectangular cross sections were used in most studies, as seen in Tables 5–13, possibly because of their simpler manufacturing process compared to other shapes.

Yogesh and Prajapati [236] conducted a numerical investigation to analyze how altering the fin height of a rectangular MCHS affects its thermo-hydro properties. They explored seven different heat sink designs in the Re range of 100–400 and the heat-flux range of 100–500 kW m⁻². Their findings indicate that raising the height of fin enhances the heat transfer from the MCHS, but only until the fin height reaches 0.8 mm. Longer fins obstruct the flow channel more, resulting in increased pressure loss. To see the effect of various crystal structure on the thermomechanical

Table 16 Investigation on various ceramic material used for construction of MCHS & MCHE

S.no.	Material	Findings	Ref.
1	Al ₂ O ₃	For mass flow rates of 20 to 120 kg h ⁻¹ , the efficacy ranged from 0.10 to 0.22 and the heat transfer coefficient extended to 22 kW m ⁻² K ⁻¹	[221]
2		Increasing the flow rate of mass reduces the pressure drop, but it also reduces the efficacy of the device	[227]
3	SiC	Heat exchangers were observed to have a massive heat transfer surface to volume ratio of 995m ³ m ⁻² and high efficacy of up to 65 percent	[222]
4		A vortex formed in the frontal area of a fin results in a notable improvement in heat transfer	[223]
5		Ceramic heat exchangers may achieve greater cycle efficiency	[224]
6		Due to an extraordinarily high coefficient of thermal conductivity of silicon carbide, the temperature gradients between channel walls was eliminated and maintains low stresses	[226]
7		A porous ceramic heat exchanger with multiple scales offers thermal performance of over 2.5 times greater than printed-circuit heat exchangers	[231]
8	SiCN	The results indicate that design optimization can improve the thermal efficiency of the cycle by nearly 9%	[225]
9	TiB ₂ -SiC doped with 2 mass% carbon fiber	TiB ₂ -SiC and TiB ₂ -SiC-Cf composites improved the heat transfer by 15.5 percent as compared to alumina	[228]
10	AlN	The effectiveness and thermal conductivity of the MCHE, which was fabricated using AlN rather than Al ₂ O ₃ , were enhanced by 26% and 59%, correspondingly	[229]
11		A reduction of approximately 31% in the overall thermal resistance of the heat sink was reported due to the higher thermal conductivity of AlN	[232]
12	ZrB ₂	The research findings indicated that the high heat transfer rate was due to the superior thermal conductivity of ceramics	[230]
13	BeO	When the mass flow rate is fixed at 30.5 kg h ⁻¹ , BeO's better thermal properties result in a more evenly distributed temperature and a 219% increase in the efficiency of MCHE with trapezoidal fins compared to MCHE made of alumina	[233]
14	AlN and BeO	When compared to alumina, AlN and BeO ceramics MCHS exhibited thermal performance improvements of about 3.72 and 4.22 times, respectively, at a Reynolds number of 300	[234]
15	ZrB ₂ -SiC-CNT	The findings indicate that the ZrB ₂ composite, which is reinforced with 20 vol.% SiC, experiences the most notable decrease in temperature when subjected to ultra-high heat flux. Subsequently, at Re 250, the ZrB ₂ composite reinforced with 20 vol.% SiC and 10 vol.% CNT also shows a considerable reduction in temperature	[235]

performance of a MCHE, a numerical experiment was conducted by Wu et al. [237]. They employed multi-physics mathematical model using thermal-fluid-structure interaction (TFSI) to investigate the thermomechanical performance of a MCHE. They found that in comparison with simple cubic crystal structure, the thermal-hydraulic performance factors of FCC and BCC corrugated straight plate MCHE were 2.20 and 1.70.

Through numerical simulations, Kumar and Kumar [238] studied the thermo-hydro properties of a rectangular MCHS featuring arc grooves on its surface. The inclusion of grooves has been observed to generate a pseudo-secondary flow, which enhances heat transfer but results in a higher Poiseuille number. Ma et al. [239] presented their findings on thermal characteristics of laminar regime in 3D microchannels having rectangular cross section, where the aspect ratios ranged from 0.1 to 1. They discovered that as the aspect ratio of rectangular microchannels increases and the Reynolds number decreases, the dimensionless thermal entry length also increases uniformly. Lan et al. [240] studied the impact of truncated and offset pin-fins on the thermal

behavior and entropy production in a rectangular MCHS that had different flow characteristics. They discovered that increasing the height of the pin-fins generally resulted in higher heat transfer but also increased fluid resistance. Kose et al. [241] conducted a numerical investigation to assess the heat transfer performance of microchannel heat sinks (MCHS) with different shapes. They compared rectangular, triangular, and trapezoidal microchannels under identical design constraints in order to determine efficient MCHS designs. The study revealed that the rectangular microchannel configuration exhibited the highest thermal and hydrodynamic performance among the three shapes. In terms of heat transfer efficiency, the rectangular microchannel required 17% and 40% less pumping power than the trapezoidal and triangular microchannels, respectively, while achieving the same amount of heat transfer. Fani et al. [242] examined how the size of particles affects the thermo-fluidic properties of nanofluids in a MCHS having trapezoidal cross section. The experiment employed CuO nanoparticles with sizes ranging from 100 to 200 nm and volume concentrations of 1% to 4%, using water as the base fluid. The findings revealed that

enlarging the nanoparticles led to a decrease in heat transfer and an increase in pressure drop. Furthermore, the base fluid had a more significant effect on the thermal performance than the nanoparticles.

Weilin et al. [243] investigated the fluidic behavior of water in microchannels constructed of silicon having trapezoidal shapes with channel diameters in the range 51–169 μm . They proposed that the equation of motion should include viscosity, specifically eddy viscosity during turbulent flow. Song et al. [244] conducted numerical simulations to investigate the thermo-fluidic properties of trapezoidal microchannel heat sinks (TMCHS). They analyzed six different configurations of TMCHS and compared their thermo-fluidic characteristics. The results showed that among the six designs, the TMCHS with the reverse channel counter-flow large inlet (RCCFLI) design had the most efficient thermal performance. Ahmed et al. [245] studied how different geometrical parameters affect the laminar flow and heat transfer performance in a grooved MCHS. They found that the trapezoidal groove MCHS had the most efficient thermal design among various grooved MCHS, with an increase in the Nu by 51.59 percent and an increase in friction factor by 2.35 percent.

Mohammed et al. [246] used numerical simulations to assess the impact of incorporating nanofluids in a parallel-flow MCHE having square cross section. Their results demonstrated that the use of nanofluids can enhance the thermal characteristics and performance of the heat exchanger, despite causing a slight increase in pressure drop. Zheng et al. [247] conducted a study on the thermo-fluidic performance of circular and annular microchannels with dimples or protrusions. They investigated the impact of various factors, including Re, size of dimples/protrusions, combinations of dimples/protrusions, and positioning patterns. Their research demonstrated that protrusions in circular microchannels are particularly beneficial for energy conservation.

The effect of particle shape on the thermo-fluidic behavior of MCHS with various geometries, i.e., circular, elliptical, triangular, and hexagonal, was studied by Monavari et al. [248]. Their findings showed that the triangular MCHS had the highest heat transfer coefficient value, followed by the elliptical, hexagonal, and circular MCHS in decreasing order. Wang et al. [249] conducted a numerical investigation on the impact of geometric factors on the thermohydraulic performance of microchannel heat sinks (MCHS) with rectangular, trapezoidal, and triangular geometries. Their research showed that the rectangular MCHS had the lowest thermal resistance among the three types, followed by the triangular and trapezoidal MCHS in increasing order of thermal resistance. In another research Tan et al. [250] conducted a numerical investigation to analyze the heat exchange mechanism and optimization of structural parameters for a built-in series combined MCHS. Through

an orthogonal test, they investigated the impact of multiple parameters on the heat exchange efficiency. The study revealed that the shape of the microchannel plays a significant role in determining the heat exchange phenomena.

Conclusions

In this study, the focus was on techniques to improve heat transfer in microchannel heat exchangers (MCHE) and microchannel heat sinks (MCHS). Various techniques were reviewed, including the utilization of different working fluids, flow disruptions, different materials for constructing microchannels, and modifications to microchannel geometries. Additionally, statistical factors such as bibliographic analyses were conducted. The main findings of the study are summarized below.

Microchannels have exceptional heat transfer properties that enable them to absorb substantial heat fluxes in very small areas. However, despite their potential, commercially available microchannels have not yet replaced conventional channels due to the high cost of the specialized manufacturing processes required to produce micro- and minichannels. Nearly half of the studies conducted on microchannel heat sinks (MCHS) and microchannel heat exchangers (MCHE) have utilized numerical approaches. In the past decade, there has been a proliferation of numerical studies, with a relative decrease in analytical and experimental research.

Although there have been notable advances in the development of microchannel heat sinks (MCHS) for electronic cooling applications, research in large-scale thermal and energy applications has been limited. In practical thermal applications, heat exchangers often incorporate core components with complex geometric designs. However, most of the studies conducted on microchannel heat exchangers (MCHE) and MCHS have focused on fundamental microchannel geometries, particularly rectangular ones, and working fluids. To accurately represent real-world heat exchangers, extensive research is required on a wide range of configurations, manifold geometries, materials, and working fluids.

Numerous studies have demonstrated that the optimal method for removing high heat flux from small volumes and spaces is by allowing the working fluid to flow through a microchannel. The addition of nanoparticles in small quantities to the base fluid can further enhance the thermal and fluid flow characteristics of the microchannel. Al_2O_3 is the most commonly used nanofluid due to its low density and high thermal conductivity. However, the use of nanofluid has a negative impact on energy consumption since it requires more electricity for pumping.

The use of flow disruption techniques, such as the wavy microchannel design, has been found to have a significant

impact on the heat transfer performance of microchannel heat sinks. The effectiveness of this technique can be attributed to three main mechanisms. Firstly, it increases the surface area available for convective heat transfer. Secondly, it alters the parabolic velocity profile, leading to improved convective heat transfer. Finally, it creates Dean vortices & chaotic advection, resulting in improved convective fluid mixing. While the wavy channel design may cause pressure losses, the benefits to heat transfer outweigh the associated pressure drop penalty.

The researchers evaluated various materials for constructing microchannels, including metals, ceramics, and polymers. Based on their findings, ceramics were determined to be the optimal material for high-temperature applications due to their ability to address metallurgical issues and corrosion problems.

Future scope

Here are some suggestions and recommendations for future work based on the published studies on heat transfer improvement in microchannel heat sinks/heat exchangers:

- (i) Use of combined active and passive techniques in microchannel heat sinks/heat exchangers for further heat transfer augmentation.
- (ii) The use of ultra-high-temperature ceramics in place of metals and superalloys in high-temperature power generating applications can solve the metallurgical constraint of the high inlet temperature of microturbines and increase the efficiency of the plant.
- (iii) The thermal performance of microchannels has to be further enhanced, and other manufacturing processes for miniaturization are needed to cut their cost.
- (iv) Further research is needed to explore the potential of nanofluids in enhancing the thermal and fluid flow characteristics of microchannels. The effects of different types and concentrations of nanoparticles, as well as their impact on pump power consumption, need to be thoroughly investigated.
- (v) More studies are needed to investigate the effects of various flow disruption techniques and microchannel geometries on heat transfer enhancement. In particular, further research should focus on exploring the performance of wavy microchannels and their potential applications in large-scale thermal and energy systems.
- (vi) Future studies should consider a wider range of working fluids to explore their potential in microchannel heat sinks/heat exchangers. Researchers should also focus on investigating the effects of fluid properties, such as viscosity and surface tension, on the thermal and fluid flow characteristics of microchannels.
- (vii) The development of advanced manufacturing techniques that can produce cost-effective and high-performance microchannel heat sinks/heat exchangers should be prioritized. This could involve exploring the use of 3D printing and other novel fabrication techniques.
- (viii) Further studies should explore the effects of operational conditions such as flow rate, inlet temperature, and pressure drop on the performance of microchannel heat sinks/heat exchangers.
- (ix) The potential of microchannel heat sinks/heat exchangers in applications beyond electronic cooling, such as in the fields of energy and biomedicine, should be explored.
- (x) Finally, researchers should focus on developing accurate numerical models and experimental methods to predict and measure the thermal and fluid flow characteristics of microchannel heat sinks/heat exchangers.

Author declaration There is no review paper which compiles all the heat transfer enhancement techniques on MCHS & MCHE. Also, information on ceramic MCHE and MCHS is limited. In this paper, the authors have tried to review all the journal papers that dealt with improvement in thermal performance of MCHS and MCHE. The effort behind this work can be divided into four main aspects: working fluid, flow disruption techniques, the material of construction, and the geometry of the channel.

References

1. Zimparov V. Energy conservation through heat transfer enhancement techniques. *Int J Energy Res.* 2002;26(7):675–96. <https://doi.org/10.1002/er.810>.
2. Mehendafe SS, Jacobi AM, Shah RK. Fluid flow and heat transfer at micro- and meso-scales with application to heat exchanger design. *Appl Mech Rev.* 2000;53(7):175–93. <https://doi.org/10.1115/1.3097347>.
3. Kandlikar SG, Grande WJ. Evolution of microchannel flow passages-thermohydraulic performance and fabrication technology. *Heat Transfer Eng.* 2003;24(1):3–17. <https://doi.org/10.1080/0145763030404040>.
4. Tuckerman DB, Pease RFW. High-performance heat sinking for VLSI. *IEEE Electron Device Lett.* 1981;2(5):126–9. <https://doi.org/10.1109/EDL.1981.25367>.
5. Steinke ME, Kandlikar SG. Single-phase liquid friction factors in microchannels. *Int J Therm Sci.* 2006;45(11):1073–83. <https://doi.org/10.1016/j.ijthermalsci.2006.01.016>.
6. Xiang J, Deng L, Zhou C, Zhao H, Huang J, Tao S. Heat transfer performance and structural optimization of a novel micro-channel heat sink. *Chin J Mech Eng (Engl Edn).* 2022;35(1):1–12. <https://doi.org/10.1186/S10033-022-00704-5/FIGURES/15>.
7. Xiong D, Azar K, Tavassoli B. High capacity, compact hybrid air cooling system. *Thermomech Phenom Electron Syst Proc Intersoc Conf.* 2006;2006(781):786–90. <https://doi.org/10.1109/ITHERM.2006.1645427>.
8. Ho C, Tai Y. Micro-electro-mechanical-systems (mems) and fluid. 1998; 579–612.
9. Peiyi W, Little WA. Measurement of friction factors for the flow of gases in very fine channels used for

- microminiature Joule-Thomson refrigerators. *Cryogenics* (Guildf). 1983;23(5):273–7. [https://doi.org/10.1016/0011-2275\(83\)90150-9](https://doi.org/10.1016/0011-2275(83)90150-9).
10. Swift G, Migliori A, Wheatley J. Microchannel crossflow fluid heat exchanger and method for its fabrication. *J Heat Recov Syst*. 1986;6(1):xiv. [https://doi.org/10.1016/0198-7593\(86\)90218-3](https://doi.org/10.1016/0198-7593(86)90218-3).
 11. Kandlikar SG. A roadmap for implementing minichannels in refrigeration and air-conditioning systems—current status and future directions. *Heat Transfer Eng*. 2007;28(12):973–85. <https://doi.org/10.1080/01457630701483497>.
 12. Bansal P, Vineyard E, Abdelaziz O. Advances in household appliances—a review. *Appl Therm Eng*. 2011;31(17–18):3748–60. <https://doi.org/10.1016/j.applthermaleng.2011.07.023>.
 13. Kim MH, Bullard CW. Performance evaluation of a window room air conditioner with microchannel condensers. *J Energy Resour Technol Trans ASME*. 2002;124(1):47–55. <https://doi.org/10.1115/1.1446072>.
 14. Qi Z, Zhao Y, Chen J. Performance enhancement study of mobile air conditioning system using microchannel heat exchangers. *Int J Refrig*. 2010;33(2):301–12. <https://doi.org/10.1016/j.ijrefrig.2009.08.014>.
 15. Hrnjak P, Litch AD. Microchannel heat exchangers for charge minimization in air-cooled ammonia condensers and chillers. *Int J Refrig*. 2008;31(4):658–68. <https://doi.org/10.1016/j.ijrefrig.2007.12.012>.
 16. Wang H, Peterson RB. Performance enhancement of a thermally activated cooling system using microchannel heat exchangers. *Appl Therm Eng*. 2011;31(14–15):2951–62. <https://doi.org/10.1016/j.applthermaleng.2011.05.026>.
 17. Barbosa JR, Ribeiro GB, de Oliveira PA. A state-of-the-art review of compact vapor compression refrigeration systems and their applications. *Heat Transfer Eng*. 2012;33(4–5):356–74. <https://doi.org/10.1080/01457632.2012.613275>.
 18. Choi SUS, Li S, Eastman JA. Measuring thermal conductivity of fluids containing oxide nanoparticles; 1999. <https://doi.org/10.1115/1.2825978>.
 19. Asadi A, et al. Recent advances in preparation methods and thermophysical properties of oil-based nanofluids: a state-of-the-art review. *Powder Technol*. 2019;352:209–26. <https://doi.org/10.1016/J.POWTEC.2019.04.054>.
 20. Said Z, Hachicha AA, Aberoumand S, Yousef BAA, Sayed ET, Bellou E. Recent advances on nanofluids for low to medium temperature solar collectors: energy, exergy, economic analysis and environmental impact. *Prog Energy Combust Sci*. 2021;84:100898. <https://doi.org/10.1016/J.PECS.2020.100898>.
 21. Aberoumand S, Jafarimoghaddam A, Moravej M, Aberoumand H, Javaherdeh K. Experimental study on the rheological behavior of silver-heat transfer oil nanofluid and suggesting two empirical based correlations for thermal conductivity and viscosity of oil based nanofluids. *Appl Therm Eng*. 2016;101:362–72. <https://doi.org/10.1016/J.APPLTHERMALENG.2016.01.148>.
 22. Aberoumand S, Jafarimoghaddam A. Experimental study on synthesis, stability, thermal conductivity and viscosity of Cu–engine oil nanofluid. *J Taiwan Inst Chem Eng*. 2017;71:315–22. <https://doi.org/10.1016/J.JTICE.2016.12.035>.
 23. Liu C, et al. Preparation and thermophysical study on a super stable copper oxide/deep eutectic solvent nanofluid. *J Mol Liq*. 2022;356:119020. <https://doi.org/10.1016/J.MOLLIQ.2022.119020>.
 24. el Mghari H, Louahli-Gualous H, Lepinasse E. Numerical study of nanofluids condensation heat transfer in a square microchannel. *Numeri Heat Transf A Appl*. 2016;69(9):957–76. <https://doi.org/10.1080/10407782.2015.1109339>.
 25. Abbassi H, Aghanajafi C. Evaluation of heat transfer augmentation in a nanofluid-cooled microchannel heat sink. *J Fusion Energy*. 2006;25(3–4):187–96. <https://doi.org/10.1007/s10894-006-9021-x>.
 26. Diao Y, Liu Y, Wang R, Zhao Y, Guo L. Experimental investigation of the Cu/R141b nanofluids on the evaporation/boiling heat transfer characteristics for surface with capillary micro-channels. *Heat and Mass Transfer/Waerme- und Stoffuebertragung*. 2014;50(9):1261–74. <https://doi.org/10.1007/s00231-014-1325-1>.
 27. Boudouh M, Gualous HL, de Labachellerie M. Local convective boiling heat transfer and pressure drop of nanofluid in narrow rectangular channels. *Appl Therm Eng*. 2010;30(17–18):2619–31. <https://doi.org/10.1016/j.applthermaleng.2010.06.027>.
 28. Hatami M, Ganji DD. Thermal and flow analysis of micro-channel heat sink (MCHS) cooled by Cu-water nanofluid using porous media approach and least square method. *Energy Convers Manag*. 2014;78:347–58. <https://doi.org/10.1016/j.enconman.2013.10.063>.
 29. Şimşek E, Coskun S, Okutucu-Özyurt T, Unalan HE. Heat transfer enhancement by silver nanowire suspensions in microchannel heat sinks. *Int J Therm Sci*. 2018;123:1–13. <https://doi.org/10.1016/j.ijthermalsci.2017.08.021>.
 30. Forghani-Tehrani P, Karimipour A, Afrand M, Mousavi S. Different nano-particles volume fraction and Hartmann number effects on flow and heat transfer of water-silver nanofluid under the variable heat flux. *Physica E Low Dimens Syst Nanostruct*. 2017;85:271–9. <https://doi.org/10.1016/j.physe.2016.07.016>.
 31. Shahsavari A, Roohani S, Jahangiri A. Evaluation of the effect of rifled inlet on the hydrothermal performance and entropy generation of biological silver/water nanofluid-cooled heatsink. *J Therm Anal Calorim*. 2022;147(20):11561–75. <https://doi.org/10.1007/S10973-022-11342-3/FIGURES/15>.
 32. Sarafraz MM, Nikkiah V, Nakhjavani M, Arya A. Thermal performance of a heat sink microchannel working with biologically produced silver-water nanofluid: experimental assessment. *Exp Therm Fluid Sci*. 2018;91:509–19. <https://doi.org/10.1016/j.expthermflusci.2017.11.007>.
 33. Behnampour A, et al. Analysis of heat transfer and nanofluid flow in microchannels with trapezoidal, rectangular and triangular shaped ribs. *Physica E Low Dimens Syst Nanostruct*. 2017;91:15–31. <https://doi.org/10.1016/j.physe.2017.04.006>.
 34. Heydari A, et al. The effect of attack angle of triangular ribs on heat transfer of nanofluids in a microchannel. *J Therm Anal Calorim*. 2018;131(3):2893–912. <https://doi.org/10.1007/s10973-017-6746-x>.
 35. Alipour H, Karimipour A, Safaei MR, Semiromi DT, Akbari OA. Influence of T-semi attached rib on turbulent flow and heat transfer parameters of a silver-water nanofluid with different volume fractions in a three-dimensional trapezoidal microchannel. *Physica E Low Dimens Syst Nanostruct*. 2017;88:60–76. <https://doi.org/10.1016/j.physe.2016.11.021>.
 36. Herrmann-Priesnitz B, Calderón-Muñoz WR, Valencia A, Soto R. Thermal design exploration of a swirl flow microchannel heat sink for high heat flux applications based on numerical simulations. *Appl Therm Eng*. 2016;109:22–34. <https://doi.org/10.1016/j.applthermaleng.2016.08.054>.
 37. Petrovic A, Lelea D, Laza I. The comparative analysis on using the NEPCM materials and nanofluids for microchannel cooling solutions. *Int Commun Heat Mass Transfer*. 2016;79:39–45. <https://doi.org/10.1016/j.icheatmasstransfer.2016.10.007>.
 38. Bhattacharya P, Samanta AN, Chakraborty S. Numerical study of conjugate heat transfer in rectangular microchannel heat sink with Al₂O₃/H₂O nanofluid. *Heat and Mass Transfer/Waerme- und Stoffuebertragung*. 2009;45(10):1323–33. <https://doi.org/10.1007/S00231-009-0510-0>.
 39. Ali AM, Rona A, Kadhim HT, Angelino M, Gao S. Thermo-hydraulic performance of a circular microchannel heat sink using

- swirl flow and nanofluid. *Appl Therm Eng.* 2021;191:116817. <https://doi.org/10.1016/j.applthermaleng.2021.116817>.
40. Heidarshenas A, Azizi Z, Peyghambarzadeh SM, Sayyahi S. Experimental investigation of heat transfer enhancement using ionic liquid-Al₂O₃ hybrid nanofluid in a cylindrical microchannel heat sink. *Appl Therm Eng.* 2021;191:116879. <https://doi.org/10.1016/j.applthermaleng.2021.116879>.
 41. Li J, Kleinstreuer C. Thermal performance of nanofluid flow in microchannels. *Int J Heat Fluid Flow.* 2008;29(4):1221–32. <https://doi.org/10.1016/j.ijheatfluidflow.2008.01.005>.
 42. Yang YT, Tsai KT, Wang YH, Lin SH. Numerical study of microchannel heat sink performance using nanofluids. *Int Commun Heat Mass Transfer.* 2014;57:27–35. <https://doi.org/10.1016/j.icheatmasstransfer.2014.07.006>.
 43. Duangthongsuk W, Wongwises S. An experimental investigation on the heat transfer and pressure drop characteristics of nanofluid flowing in microchannel heat sink with multiple zigzag flow channel structures. *Exp Therm Fluid Sci.* 2017;87:30–9. <https://doi.org/10.1016/j.expthermflusci.2017.04.013>.
 44. Martínez VA, Lozano-Steinmetz F, Vasco DA, Zapata PA, Chi-Durán I, Singh DP. Thermal characterization and stability analysis of aqueous ZnO-based nanofluids numerically implemented in microchannel heat sinks. *Thermal Sci Eng Prog.* 2021;22:100792. <https://doi.org/10.1016/j.tsep.2020.100792>.
 45. Mohammed HA, Gunnasegaran P, Shuaib NH. The impact of various nanofluid types on triangular microchannels heat sink cooling performance. *Int Commun Heat Mass Transfer.* 2011;38(6):767–73. <https://doi.org/10.1016/j.icheatmasstransfer.2011.03.024>.
 46. Salman BH, Mohammed HA, Kherbeet AS. Heat transfer enhancement of nanofluids flow in microtube with constant heat flux. *Int Commun Heat Mass Transfer.* 2012;39(8):1195–204. <https://doi.org/10.1016/j.icheatmasstransfer.2012.07.005>.
 47. Nebbati R, Kadja M. Study of forced convection of a nanofluid used as a heat carrier in a microchannel heat sink. In *Energy Procedia*, Elsevier Ltd; 2015, pp. 633–642. <https://doi.org/10.1016/j.egypro.2015.07.799>.
 48. Mirzaei M, Dehghan M. Investigation of flow and heat transfer of nanofluid in microchannel with variable property approach. *Heat Mass Transfer.* 2013;49(12):1803–11. <https://doi.org/10.1007/s00231-013-1217-9>.
 49. Zhang Z, Xie Y, Zhang D, Xie G. Flow characteristic and heat transfer for non-newtonian nanofluid in rectangular microchannels with teardrop dimples/protrusions. *Open Physics.* 2017;15(1):197–206. <https://doi.org/10.1515/phys-2017-0021>.
 50. Wang R, Du J, Zhu Z. Effects of wall slip and nanoparticles' thermophoresis on the convective heat transfer enhancement of nanofluid in a microchannel. *J Therm Sci Technol.* 2016;11:1. <https://doi.org/10.1299/jtst.2016jtst00017>.
 51. Shamsi MR, Akbari OA, Marzban A, Toghraie D, Mashayekhi R. Increasing heat transfer of non-Newtonian nanofluid in rectangular microchannel with triangular ribs. *Physica E Low Dimens Syst Nanostruct.* 2017;93:167–78. <https://doi.org/10.1016/j.physe.2017.06.015>.
 52. Yang YT, Tang HW, Ding WP. Optimization design of microchannel heat sink using nanofluid by numerical simulation coupled with genetic algorithm. *Int Commun Heat Mass Transfer.* 2016;72:29–38. <https://doi.org/10.1016/j.icheatmasstransfer.2016.01.012>.
 53. Wu J, Zhao J, Lei J, Liu B. Effectiveness of nanofluid on improving the performance of microchannel heat sink. *Appl Therm Eng.* 2016;101:402–12. <https://doi.org/10.1016/j.applthermaleng.2016.01.114>.
 54. Kalteh M, Abbassi A, Saffar-Avval M, Frijns A, Darhuber A, Harting J. Experimental and numerical investigation of nanofluid forced convection inside a wide microchannel heat sink. *Appl Therm Eng.* 2012;36(1):260–8. <https://doi.org/10.1016/j.applthermaleng.2011.10.023>.
 55. Rahmati AR, Azizi T, Mousavi SH, Zarareh A. Boundaries on mixed convection of Al₂O₃-water nanofluid in microcavity; 2015.
 56. Mohammed HA, Gunnasegaran P, Shuaib NH. Heat transfer in rectangular microchannels heat sink using nanofluids. *Int Commun Heat Mass Transfer.* 2010;37(10):1496–503. <https://doi.org/10.1016/j.icheatmasstransfer.2010.08.020>.
 57. Maganti LS, Dhar P. Consequences of flow configuration and nanofluid transport on entropy generation in parallel microchannel cooling systems. *Int J Heat Mass Transf.* 2017;109:555–63. <https://doi.org/10.1016/j.ijheatmasstransfer.2017.02.036>.
 58. Wang XD, Bin A, Xu JL. Optimal geometric structure for nanofluid-cooled microchannel heat sink under various constraint conditions. *Energy Convers Manag.* 2013;65:528–38. <https://doi.org/10.1016/j.enconman.2012.08.018>.
 59. Akbari OA, Toghraie D, Karimipour A, Marzban A, Ahmadi GR. The effect of velocity and dimension of solid nanoparticles on heat transfer in non-Newtonian nanofluid. *Physica E Low Dimens Syst Nanostruct.* 2017;86:68–75. <https://doi.org/10.1016/j.physe.2016.10.013>.
 60. Mohammadian SK, Seyf HR, Zhang Y. Performance augmentation and optimization of aluminum oxide-water nanofluid flow in a two-fluid microchannel heat exchanger. *J Heat Transfer.* 2014;136:2. <https://doi.org/10.1115/1.4025431>.
 61. Chen CH, Ding CY. Study on the thermal behavior and cooling performance of a nanofluid-cooled microchannel heat sink. *Int J Therm Sci.* 2011;50(3):378–84. <https://doi.org/10.1016/j.jtthermalsci.2010.04.020>.
 62. Soltanipour H, Khalilarya S, Yekani Motlagh S, Mirzaei I. The effect of position-dependent magnetic field on nanofluid forced convective heat transfer and entropy generation in a microchannel. *J Braz Soc Mech Sci Eng.* 2017;39(1):345–55. <https://doi.org/10.1007/s40430-016-0541-7>.
 63. Abdollahi A, Sharma RN, Mohammed HA, Vatani A. Heat transfer and flow analysis of Al₂O₃-Water nanofluids in interrupted microchannel heat sink with ellipse and diamond ribs in the transverse microchambers. *Heat Transfer Eng.* 2018;39(16):1461–9. <https://doi.org/10.1080/01457632.2017.1379344>.
 64. Akbarinia A, Abdolzadeh M, Laur R. Critical investigation of heat transfer enhancement using nanofluids in microchannels with slip and non-slip flow regimes. *Appl Therm Eng.* 2011;31(4):556–65. <https://doi.org/10.1016/j.applthermaleng.2010.10.017>.
 65. Kalteh M, Abedinzadeh SS. Numerical investigation of MHD nanofluid forced convection in a microchannel using lattice Boltzmann method. *Iran J Sci Technol Trans Mech Eng.* 2018;42(1):23–34. <https://doi.org/10.1007/s40997-017-0073-5>.
 66. Patel VU, Modi AJ, Professor A, Bardoli C, Assistant Professor G, Bhuj G. IJESRT International Journal of Engineering Sciences & Research Technology Analysis of Microchannel Heat Sink Using Cfd. No. 6, 2015, Accessed: Jun. 27, 2021. [Online]. www.ijesrt.com
 67. Akbari OA, Toghraie D, Karimipour A. Impact of ribs on flow parameters and laminar heat transfer of water-aluminum oxide nanofluid with different nanoparticle volume fractions in a three-dimensional rectangular microchannel. *Adv Mech Eng.* 2015. <https://doi.org/10.1177/1687814015618155>.
 68. Shi X, Li S, Wei Y, Gao J. Numerical investigation of laminar convective heat transfer and pressure drop of water-based Al₂O₃ nanofluids in a microchannel. *Int Commun Heat Mass Transfer.* 2018;90:111–20. <https://doi.org/10.1016/j.icheatmasstransfer.2017.11.007>.

69. Elbadawy I, Fayed M. Reliability of Al₂O₃ nanofluid concentration on the heat transfer augmentation and resizing for single and double stack microchannels. *Alex Eng J.* 2020;59(3):1771–85. <https://doi.org/10.1016/j.aej.2020.04.046>.
70. Parsaiemehr M, Pourfattah F, Akbari OA, Toghraie D, Sheikhzadeh G. Turbulent flow and heat transfer of Water/Al₂O₃ nanofluid inside a rectangular ribbed channel. *Physica E Low Dimens Syst Nanostruct.* 2018;96:73–84. <https://doi.org/10.1016/j.physe.2017.10.012>.
71. Ting TW, Hung YM, Guo N. Viscous dissipative forced convection in thermal non-equilibrium nanofluid-saturated porous media embedded in microchannels. *Int Commun Heat Mass Transfer.* 2014;57:309–18. <https://doi.org/10.1016/j.icheatmasstransfer.2014.08.018>.
72. Anbumeenakshi C, Thansekhar MR. On the effectiveness of a nanofluid cooled microchannel heat sink under non-uniform heating condition. *Appl Therm Eng.* 2017;113:1437–43. <https://doi.org/10.1016/j.applthermaleng.2016.11.144>.
73. Ghale ZY, Haghshenasfard M, Esfahany MN. Investigation of nanofluids heat transfer in a ribbed microchannel heat sink using single-phase and multiphase CFD models. *Int Commun Heat Mass Transfer.* 2015;68:122–9. <https://doi.org/10.1016/j.icheatmasstransfer.2015.08.012>.
74. Xu L, Xu J. Nanofluid stabilizes and enhances convective boiling heat transfer in a single microchannel. *Int J Heat Mass Transf.* 2012;55(21–22):5673–86. <https://doi.org/10.1016/j.ijheatmasstransfer.2012.05.063>.
75. Ho CJ, Wei LC, Li ZW. An experimental investigation of forced convective cooling performance of a microchannel heat sink with Al₂O₃/water nanofluid. *Appl Therm Eng.* 2010;30(2–3):96–103. <https://doi.org/10.1016/j.applthermaleng.2009.07.003>.
76. Saini A, Sharma S, Gangacharyulu D. Study of heat transfer of aluminium oxide nanofluids using aluminium split flow microchannels; 2016. <https://doi.org/10.17577/ijertv5is070339>.
77. Vafaei S, Wen D. Flow boiling heat transfer of alumina nanofluids in single microchannels and the roles of nanoparticles. *J Nanopart Res.* 2011;13(3):1063–73. <https://doi.org/10.1007/s11051-010-0095-z>.
78. Malvandi A, Zamani M, Hosseini SJ, Moshizi SA. Figure of merit for optimization of nanofluid flow in circular microchannel by adapting nanoparticle migration. *Appl Therm Eng.* 2017;118:328–38. <https://doi.org/10.1016/j.applthermaleng.2017.02.081>.
79. Trinavee K, Gogoi TK, Pandey M. Laminar convective heat transfer characteristic of Al₂O₃/water nanofluid in a circular microchannel. In: *Journal of Physics: Conference Series Institute of Physics Publishing.* 2016. <https://doi.org/10.1088/1742-6596/759/1/012088>.
80. Lelea D, Laza I. The water based Al₂O₃ nanofluid flow and heat transfer in tangential microtube heat sink with multiple inlets. *Int J Heat Mass Transf.* 2014;69:264–75. <https://doi.org/10.1016/j.ijheatmasstransfer.2013.10.026>.
81. Shalchi-Tabrizi A, Seyf HR. Analysis of entropy generation and convective heat transfer of Al₂O₃ nanofluid flow in a tangential micro heat sink. *Int J Heat Mass Transf.* 2012;55(15–16):4366–75. <https://doi.org/10.1016/j.ijheatmasstransfer.2012.04.005>.
82. Yao P, Zhai Y, Ma M, Li Y, Wang H. An improving performance evaluation plot (PEP) for energy management in microchannel heat sinks by using nanofluids. *Int Commun Heat Mass Transfer.* 2020;117:104808. <https://doi.org/10.1016/j.icheatmasstransfer.2020.104808>.
83. Zhang B, Zhu J, Gao L. Topology optimization design of nanofluid-cooled microchannel heat sink with temperature-dependent fluid properties. *Appl Therm Eng.* 2020;176:115354. <https://doi.org/10.1016/j.applthermaleng.2020.115354>.
84. Kumar R, Arjun KS, Rakesh K. Heat transfer enhancement using alumina nanofluid in circular micro channel. *Numerical Simulations of Heat Transfer Enhancement in Flowing Nanofluids View project Designs using CFD Tools View project Arjun Sunil Indian Institute of Technology (ISM) Dhanbad; 2017.* Accessed 29 Jun 2021. [Online]. <https://www.researchgate.net/publication/316548232>
85. Lee J, Mudawar I. Assessment of the effectiveness of nanofluids for single-phase and two-phase heat transfer in micro-channels. *Int J Heat Mass Transf.* 2007;50(3–4):452–63. <https://doi.org/10.1016/j.ijheatmasstransfer.2006.08.001>.
86. Zhang H, Shao S, Xu H, Tian C. Heat transfer and flow features of Al₂O₃-water nanofluids flowing through a circular microchannel—experimental results and correlations. *Appl Therm Eng.* 2013;61(2):86–92. <https://doi.org/10.1016/j.applthermaleng.2013.07.026>.
87. Hedayati F, Malvandi A, Kaffash MH, Ganji DD. Fully developed forced convection of alumina/water nanofluid inside microchannels with asymmetric heating. *Powder Technol.* 2015;269:520–31. <https://doi.org/10.1016/j.powtec.2014.09.034>.
88. López A, Ibáñez G, Pantoja J, Moreira J, Lastres O. Entropy generation analysis of MHD nanofluid flow in a porous vertical microchannel with nonlinear thermal radiation, slip flow and convective-radiative boundary conditions. *Int J Heat Mass Transf.* 2017;107:982–94. <https://doi.org/10.1016/j.ijheatmasstransfer.2016.10.126>.
89. Baheri Islami S, Dastvareh B, Gharraei R. An investigation on the hydrodynamic and heat transfer of nanofluid flow, with non-Newtonian base fluid, in micromixers. *Int J Heat Mass Transf.* 2014;78:917–29. <https://doi.org/10.1016/j.ijheatmasstransfer.2014.07.022>.
90. Yang YT, Lai FH. Numerical study of flow and heat transfer characteristics of alumina-water nanofluids in a microchannel using the lattice Boltzmann method. *Int Commun Heat Mass Transfer.* 2011;38(5):607–14. <https://doi.org/10.1016/j.icheatmasstransfer.2011.03.010>.
91. Ganguly S, Sarkar S, Kumar Hota T, Mishra M. Thermally developing combined electroosmotic and pressure-driven flow of nanofluids in a microchannel under the effect of magnetic field. *Chem Eng Sci.* 2015;126:10–21. <https://doi.org/10.1016/j.ces.2014.11.060>.
92. Moshizi SA, Malvandi A. Magnetic field effects on nanoparticle migration at mixed convection of MHD nanofluids flow in microchannels with temperature-dependent thermophysical properties. *J Taiwan Inst Chem Eng.* 2016;66:269–82. <https://doi.org/10.1016/j.jtice.2016.06.036>.
93. Ting TW, Hung YM, Guo N. Viscous dissipative nanofluid convection in asymmetrically heated porous microchannels with solid-phase heat generation. *Int Commun Heat Mass Transfer.* 2015;68:236–47. <https://doi.org/10.1016/j.icheatmasstransfer.2015.09.003>.
94. Mah WH, Hung YM, Guo N. Entropy generation of viscous dissipative nanofluid flow in microchannels. *Int J Heat Mass Transf.* 2012;55(15–16):4169–82. <https://doi.org/10.1016/j.ijheatmasstransfer.2012.03.058>.
95. Malvandi A, Moshizi SA, Ganji DD. Effects of temperature-dependent thermophysical properties on nanoparticle migration at mixed convection of nanofluids in vertical microchannels. *Powder Technol.* 2016;303:7–19. <https://doi.org/10.1016/j.powtec.2016.08.063>.
96. Malvandi A, Moshizi SA, Ganji DD. Two-component heterogeneous mixed convection of alumina/water nanofluid in microchannels with heat source/sink. *Adv Powder Technol.* 2016;27(1):245–54. <https://doi.org/10.1016/j.apt.2015.12.009>.
97. Zhao G, Jian Y, Li F. Streaming potential and heat transfer of nanofluids in parallel plate microchannels. *Colloids Surf A*

- Physicochem Eng Asp. 2016;498:239–47. <https://doi.org/10.1016/j.colsurfa.2016.03.053>.
98. Jung JY, Oh HS, Kwak HY. Forced convective heat transfer of nanofluids in microchannels. In: American Society of Mechanical Engineers, Heat Transfer Division, (Publication) HTD American Society of Mechanical Engineers (ASME). 2006. <https://doi.org/10.1115/IMECE2006-13851>.
 99. Ahmed M, Eslamian M. Laminar forced convection of a nanofluid in a microchannel: effect of flow inertia and external forces on heat transfer and fluid flow characteristics. *Appl Therm Eng*. 2015;78:326–38. <https://doi.org/10.1016/j.applthermaleng.2014.12.069>.
 100. Nouri D, Pasandideh-Fard M, Javad Oboodi M, Mahian O, Sahin AZ. Entropy generation analysis of nanofluid flow over a spherical heat source inside a channel with sudden expansion and contraction. *Int J Heat Mass Transf*. 2018;116:1036–43. <https://doi.org/10.1016/j.ijheatmasstransfer.2017.09.097>.
 101. Ghazvini M, Shokouhmand H. Investigation of a nanofluid-cooled microchannel heat sink using Fin and porous media approaches. *Energy Convers Manag*. 2009;50(9):2373–80. <https://doi.org/10.1016/j.enconman.2009.05.021>.
 102. Akbari OA, Toghraie D, Karimipour A. Numerical simulation of heat transfer and turbulent flow of water nanofluids copper oxide in rectangular microchannel with semi-attached rib. *Adv Mech Eng*. 2016;8(4):1–25. <https://doi.org/10.1177/1687814016641016>.
 103. Chein R, Chuang J. Experimental microchannel heat sink performance studies using nanofluids. *Int J Therm Sci*. 2007;46(1):57–66. <https://doi.org/10.1016/j.ijthermalsci.2006.03.009>.
 104. Chabi AR, Zarrinabadi S, Peyghambarzadeh SM, Hashemabadi SH, Salimi M. Local convective heat transfer coefficient and friction factor of CuO/water nanofluid in a microchannel heat sink. *Heat Mass Transfer*. 2017;53(2):661–71. <https://doi.org/10.1007/s00231-016-1851-0>.
 105. Rimbault B, Nguyen CT, Galanis N. Experimental investigation of CuO-water nanofluid flow and heat transfer inside a microchannel heat sink. *Int J Therm Sci*. 2014;84:275–92. <https://doi.org/10.1016/j.ijthermalsci.2014.05.025>.
 106. Cruz-Duarte JM, Garcia-Perez A, Amaya-Contreras IM, Correa-Cely CR. Designing a microchannel heat sink with colloidal coolants through the entropy generation minimisation criterion and global optimisation algorithms. *Appl Therm Eng*. 2016;100:1052–62. <https://doi.org/10.1016/j.applthermaleng.2016.02.109>.
 107. Sabaghan A, Edalatpour M, Moghadam MC, Roohi E, Niazmand H. Nanofluid flow and heat transfer in a microchannel with longitudinal vortex generators: two-phase numerical simulation. *Appl Therm Eng*. 2016;100:179–89. <https://doi.org/10.1016/j.applthermaleng.2016.02.020>.
 108. Martínez VA, Vasco DA, García-Herrera CM, Ortega-Aguilera R. Numerical study of TiO₂-based nanofluids flow in microchannel heat sinks: effect of the Reynolds number and the microchannel height. *Appl Therm Eng*. 2019;161:114130. <https://doi.org/10.1016/j.applthermaleng.2019.114130>.
 109. Manay E, Sahin B. The effect of microchannel height on performance of nanofluids. *Int J Heat Mass Transf*. 2016;95:307–20. <https://doi.org/10.1016/j.ijheatmasstransfer.2015.12.015>.
 110. Manay E, Sahin B. Heat transfer and pressure drop of nanofluids in a microchannel heat sink. *Heat Transfer Eng*. 2017;38(5):510–22. <https://doi.org/10.1080/10407782.2016.1195162>.
 111. Nitiapiruk P, Mahian O, Dalkilic AS, Wongwises S. Performance characteristics of a microchannel heat sink using TiO₂/water nanofluid and different thermophysical models. *Int Commun Heat Mass Transfer*. 2013;47:98–104. <https://doi.org/10.1016/j.icheatmasstransfer.2013.07.001>.
 112. Murshed SMS, Tan SH, Nguyen NT, Wong TN, Yobas L. Microdroplet formation of water and nanofluids in heat-induced microfluidic T-junction. *Microfluid Nanofluidics*. 2009;6(2):253–9. <https://doi.org/10.1007/s10404-008-0323-3>.
 113. Vinoth R, Senthil Kumar D. Channel cross section effect on heat transfer performance of oblique finned microchannel heat sink. *Int Commun Heat Mass Transfer*. 2017;87:270–6. <https://doi.org/10.1016/j.icheatmasstransfer.2017.03.016>.
 114. Wu X, Wu H, Cheng P. Pressure drop and heat transfer of Al₂O₃-H₂O nanofluids through silicon microchannels. *J Micromech Microeng*. 2009. <https://doi.org/10.1088/0960-1317/19/10/105020>.
 115. Azizi Z, Alamdari A, Malayeri MR. Convective heat transfer of Cu-water nanofluid in a cylindrical microchannel heat sink. *Energy Convers Manag*. 2015;101:515–24. <https://doi.org/10.1016/j.enconman.2015.05.073>.
 116. Azizi Z, Alamdari A, Malayeri MR. Thermal performance and friction factor of a cylindrical microchannel heat sink cooled by Cu-water nanofluid. *Appl Therm Eng*. 2016;99:970–8. <https://doi.org/10.1016/j.applthermaleng.2016.01.140>.
 117. Topuz A, Engin T, Alper Özalp A, Erdoğan B, Mert S, Yeter A. Experimental investigation of optimum thermal performance and pressure drop of water-based Al₂O₃, TiO₂ and ZnO nanofluids flowing inside a circular microchannel. *J Therm Anal Calorim*. 2018;131(3):2843–63. <https://doi.org/10.1007/s10973-017-6790-6>.
 118. Chevalier J, Tillement O, Ayela F. Rheological properties of nanofluids flowing through microchannels. *Appl Phys Lett*. 2007. <https://doi.org/10.1063/1.2821117>.
 119. Putra N, Septiadi WN, Julian G, Maulana A, Irwansyah R. An experimental study on thermal performance of nano fluids in microchannel heat exchanger. *Int J Technol*. 2013;4(2):167–77. <https://doi.org/10.14716/ijtech.v4i2.126>.
 120. Thansekhar MR, Anbumeenakshi C. Experimental investigation of thermal performance of microchannel heat sink with nanofluids Al₂O₃/water and SiO₂/water. *Exp Tech*. 2017;41(4):399–406. <https://doi.org/10.1007/s40799-017-0189-y>.
 121. Abdulbari HA, Ming FLW. Drag reduction properties of Nanofluids in microchannels. *J Eng Res*. 2015;12(2):60–7. <https://doi.org/10.24200/tjer.vol12iss2pp60-67>.
 122. Xia GD, Liu R, Wang J, Du M. The characteristics of convective heat transfer in microchannel heat sinks using Al₂O₃ and TiO₂ nanofluids. *Int Commun Heat Mass Transfer*. 2016;76:256–64. <https://doi.org/10.1016/j.icheatmasstransfer.2016.05.034>.
 123. Fani B, Kalteh M, Abbassi A. Investigating the effect of Brownian motion and viscous dissipation on the nanofluid heat transfer in a trapezoidal microchannel heat sink. *Adv Powder Technol*. 2015;26(1):83–90. <https://doi.org/10.1016/j.appt.2014.08.009>.
 124. Tran N, Chang YJ, Wang CC. Optimization of thermal performance of multi-nozzle trapezoidal microchannel heat sinks by using nanofluids of Al₂O₃ and TiO₂. *Int J Heat Mass Transf*. 2018;117:787–98. <https://doi.org/10.1016/j.ijheatmasstransfer.2017.10.051>.
 125. Narrein K, Sivasankaran S, Ganesan P. Two-phase analysis of a helical microchannel heat sink using nanofluids. *Numeri Heat Transf A Appl*. 2015;68(11):1266–79. <https://doi.org/10.1080/10407782.2015.1032017>.
 126. Mohsenian S, Ramiar A, Ranjbar AA. Numerical investigation of non-Newtonian nanofluid flow in a converging microchannel. *J Mech Sci Technol*. 2017;31(1):385–91. <https://doi.org/10.1007/s12206-016-1240-0>.
 127. Kalteh M. Investigating the effect of various nanoparticle and base liquid types on the nanofluids heat and fluid flow in a microchannel. *Appl Math Model*. 2013;37(18–19):8600–9. <https://doi.org/10.1016/j.apm.2013.03.067>.

128. Akademia Baru P, Abubakar SB, Sidik NAC. Numerical prediction of laminar nanofluid flow in rectangular microchannel heat sink; 2015. Accessed: 30 Jun 2021. [Online]. <https://akademiabaru.com/submit/index.php/arfmts/article/view/2032>
129. Abubakar S, Azwadi CSN, Ahmad A. The use of Fe₃O₄-H₂O₄ nanofluid for heat transfer enhancement in rectangular microchannel heatsink. 2016. Accessed: 30 Jun 2021. [Online]. https://sci-hub.do/https://www.akademiabaru.com/doc/ARMSV23_N1_P15_24.pdf
130. Nasiri M, Rashidi MM, Lorenzini G. Effect of magnetic field on entropy generation in a microchannel heat sink with offset fan shaped. *Entropy*. 2016;18:1. <https://doi.org/10.3390/e18010010>.
131. Adham AM, Mohd-Ghazali N, Ahmad R. Optimization of nanofluid-cooled microchannel heat sink. *Therm Sci*. 2016;20(1):109–18. <https://doi.org/10.2298/TSCI130517163A>.
132. Radwan A, Ahmed M, Ookawara S. Performance enhancement of concentrated photovoltaic systems using a microchannel heat sink with nanofluids. *Energy Convers Manag*. 2016;119:289–303. <https://doi.org/10.1016/j.enconman.2016.04.045>.
133. Paula Turcu R et al. New polypyrrole-multiwall carbon nanotubes hybrid materials Structure-property characteristics of graphene materials with controlled nanoscale rippling View project Modified titania films for photocatalysis View project New polypyrrole-multiwall carbon na; 2015. Accessed: 02 Jul 2021. [Online]. <https://www.researchgate.net/publication/266224651>
134. Jha N, Ramaprabhu S. Thermal conductivity studies of metal dispersed multiwalled carbon nanotubes in water and ethylene glycol based nanofluids. *J Appl Phys*. 2009. <https://doi.org/10.1063/1.3240307>.
135. Suresh S, Venkataraj KP, Selvakumar P, Chandrasekar M. Synthesis of Al₂O₃-Cu/water hybrid nanofluids using two step method and its thermo physical properties. *Colloids Surf A Physicochem Eng Asp*. 2011;388(1–3):41–8. <https://doi.org/10.1016/j.colsurfa.2011.08.005>.
136. Huang Y, Zou C, Chen M, Sun H. Thermophysical property evaluation of β -cyclodextrin modified ZrO₂ nanofluids for microchannel heat exchange. *Ceram Int*. 2022;48(21):31728–37. <https://doi.org/10.1016/j.ceramint.2022.07.096>.
137. Mansouri R, Pourrajab R, Behbahani M, Daneh-Dezfuli A. Evaluating the convective heat transfer of graphene oxide-gold hybrid nanofluid flow in CPU. *J Therm Anal Calorim*. 2023;148(12):5765–76. <https://doi.org/10.1007/S10973-023-12064-W/FIGURES/12>.
138. Srivastava K, Sahoo RR. Thermal, exergetic, and performance analysis of dissimilar-shaped nanoparticles hybrid nanofluid for flow across minichannel heat sink. *J Therm Anal Calorim*. 2023;148(14):7501–18. <https://doi.org/10.1007/S10973-023-12191-4/TABLES/7>.
139. Sheikhalipour T, Abbassi A. Numerical investigation of nanofluid heat transfer inside trapezoidal microchannels using a novel dispersion model. *Adv Powder Technol*. 2016;27(4):1464–72. <https://doi.org/10.1016/j.apt.2016.05.006>.
140. Seyf HR, Keshavarz Mohammadian S. Thermal and hydraulic performance of counterflow microchannel heat exchangers with and without nanofluids. *J Heat Transfer*. 2011. <https://doi.org/10.1115/1.4003553>.
141. Esmailnejad A, Aminfar H, Neistanak MS. Numerical investigation of forced convection heat transfer through microchannels with non-Newtonian nanofluids. *Int J Therm Sci*. 2014;75:76–86. <https://doi.org/10.1016/j.ijthermalsci.2013.07.020>.
142. Ebrahimi A, Rikhtegar F, Sabaghan A, Roohi E. Heat transfer and entropy generation in a microchannel with longitudinal vortex generators using nanofluids. *Energy*. 2016;101:190–201. <https://doi.org/10.1016/j.energy.2016.01.102>.
143. Pourmehran O, Rahimi-Gorji M, Hatami M, Sahebi SAR, Domairry G. Numerical optimization of microchannel heat sink (MCHS) performance cooled by KKL based nanofluids in saturated porous medium. *J Taiwan Inst Chem Eng*. 2015;55:49–68. <https://doi.org/10.1016/j.jtice.2015.04.016>.
144. Hasan MI, Rageb AMAR, Yaghoubi M. Investigation of a counter flow microchannel heat exchanger performance with using nanofluid as a coolant. *J Electron Cool Thermal Control*. 2012;02(03):35–43. <https://doi.org/10.4236/jectc.2012.23004>.
145. Jang SP, Choi SUS. Cooling performance of a microchannel heat sink with nanofluids. *Appl Therm Eng*. 2006;26(17–18):2457–63. <https://doi.org/10.1016/j.applthermaleng.2006.02.036>.
146. Kuppusamy NR, Mohammed HA, Lim CW. Numerical investigation of trapezoidal grooved microchannel heat sink using nanofluids. *Thermochim Acta*. 2013;573:39–56. <https://doi.org/10.1016/j.tca.2013.09.011>.
147. Seyf HR, Feizbakhshi M. Computational analysis of nanofluid effects on convective heat transfer enhancement of micro-pin-fin heat sinks. *Int J Therm Sci*. 2012;58:168–79. <https://doi.org/10.1016/j.ijthermalsci.2012.02.018>.
148. Karimipour A, D'Orazio A, Shadloo MS. The effects of different nano particles of Al₂O₃ and Ag on the MHD nano fluid flow and heat transfer in a microchannel including slip velocity and temperature jump. *Physica E Low Dimens Syst Nanostruct*. 2017;86:146–53. <https://doi.org/10.1016/j.physe.2016.10.015>.
149. Wu W, et al. Heat transfer enhancement of PAO in microchannel heat exchanger using nano-encapsulated phase change indium particles. *Int J Heat Mass Transf*. 2013;58(1–2):348–55. <https://doi.org/10.1016/j.ijheatmasstransfer.2012.11.032>.
150. Peyghambarzadeh SM, Hashemabadi SH, Chabi AR, Salimi M. Performance of water based CuO and Al₂O₃ nanofluids in a Cu-Be alloy heat sink with rectangular microchannels. *Energy Convers Manag*. 2014;86:28–38. <https://doi.org/10.1016/j.enconman.2014.05.013>.
151. Sivakumar A, Alagumurthi N, Senthilvelan T. Experimental investigation of forced convective heat transfer performance in nanofluids of Al₂O₃/water and CuO/water in a serpentine shaped micro channel heat sink. *Heat Mass Transfer*. 2016;52(7):1265–74. <https://doi.org/10.1007/s00231-015-1649-5>.
152. Hosseini SR, Sheikholeslami M, Ghasemian M, Ganji DD. Nanofluid heat transfer analysis in a microchannel heat sink (MCHS) under the effect of magnetic field by means of KKL model. *Powder Technol*. 2018;324:36–47. <https://doi.org/10.1016/j.powtec.2017.10.043>.
153. Rahimi-Gorji M, Pourmehran O, Hatami M, Ganji DD. Statistical optimization of microchannel heat sink (MCHS) geometry cooled by different nanofluids using RSM analysis. *Eur Phys J Plus*. 2015;130(2):1–21. <https://doi.org/10.1140/epjp/i2015-15022-8>.
154. Sohel MR, Saidur R, Hassan NH, Elias MM, Khaleduzzaman SS, Mahbulul IM. Analysis of entropy generation using nanofluid flow through the circular microchannel and minichannel heat sink. *Int Commun Heat Mass Transfer*. 2013;46:85–91. <https://doi.org/10.1016/j.icheatmasstransfer.2013.05.011>.
155. Ebrahimi S, Sabbaghzadeh J, Lajevardi M, Hadi I. Cooling performance of a microchannel heat sink with nanofluids containing cylindrical nanoparticles (carbon nanotubes). *Heat Mass Transfer*. 2010;46(5):549–53. <https://doi.org/10.1007/s00231-010-0599-1>.
156. Arabpour A, Karimipour A, Toghraie D. The study of heat transfer and laminar flow of kerosene/multi-walled carbon nanotubes (MWCNTs) nanofluid in the microchannel heat sink with slip boundary condition. *J Therm Anal Calorim*. 2018;131(2):1553–66. <https://doi.org/10.1007/s10973-017-6649-x>.
157. Nojoomizadeh M, Karimipour A. The effects of porosity and permeability on fluid flow and heat transfer of multi walled carbon nano-tubes suspended in oil (MWCNT/Oil nano-fluid) in a microchannel filled with a porous medium. *Physica E Low*

- Dimens Syst Nanostruct. 2016;84:423–33. <https://doi.org/10.1016/j.physe.2016.07.020>.
158. Nikkha Z, et al. Forced convective heat transfer of water/functionalized multi-walled carbon nanotube nanofluids in a microchannel with oscillating heat flux and slip boundary condition. *Int Commun Heat Mass Transfer*. 2015;68:69–77. <https://doi.org/10.1016/j.icheatmasstransfer.2015.08.008>.
 159. Mehraban Rad P, Aghanajafi C. The effect of thermal radiation on nanofluid cooled microchannels. *J Fusion Energy*. 2009;28(1):91–100. <https://doi.org/10.1007/s10894-008-9153-2>.
 160. Arabpour A, Karimipour A, Toghraie D, Akbari OA. Investigation into the effects of slip boundary condition on nanofluid flow in a double-layer microchannel. *J Therm Anal Calorim*. 2018;131(3):2975–91. <https://doi.org/10.1007/s10973-017-6813-3>.
 161. Mazlam NAFN, Mohd-Ghazali N, Mare T, Estelle P, Halelfadl S. Thermal and hydrodynamic performance of a microchannel heat sink cooled with carbon nanotubes nanofluid. *J Teknol*. 2016;78(10–2):69–77. <https://doi.org/10.11113/jt.v78.9670>.
 162. Nojoomizadeh M, D’Orazio A, Karimipour A, Afrand M, Goodarzi M. Investigation of permeability effect on slip velocity and temperature jump boundary conditions for FMWNT/Water nanofluid flow and heat transfer inside a microchannel filled by a porous media. *Physica E Low Dimens Syst Nanostruct*. 2018;97:226–38. <https://doi.org/10.1016/j.physe.2017.11.008>.
 163. Halelfadl S, Adham AM, Mohd-Ghazali N, Maré T, Estellé P, Ahmad R. Optimization of thermal performances and pressure drop of rectangular microchannel heat sink using aqueous carbon nanotubes based nanofluid. *Appl Therm Eng*. 2014;62(2):492–9. <https://doi.org/10.1016/j.applthermaleng.2013.08.005>.
 164. Sarafraz MM, Nikkha V, Nakhjavani M, Arya A. Fouling formation and thermal performance of aqueous carbon nanotube nanofluid in a heat sink with rectangular parallel microchannel. *Appl Therm Eng*. 2017;123:29–39. <https://doi.org/10.1016/j.applthermaleng.2017.05.056>.
 165. Sui Y, Teo CJ, Lee PS, Chew YT, Shu C. Fluid flow and heat transfer in wavy microchannels. *Int J Heat Mass Transf*. 2010;53(13–14):2760–72. <https://doi.org/10.1016/j.ijheatmasstransfer.2010.02.022>.
 166. Sui Y, Lee PS, Teo CJ. An experimental study of flow friction and heat transfer in wavy microchannels with rectangular cross section. *Int J Therm Sci*. 2011;50(12):2473–82. <https://doi.org/10.1016/j.ijthermalsci.2011.06.017>.
 167. Mohammed HA, Gunnasegaran P, Shuaib NH. Numerical simulation of heat transfer enhancement in wavy microchannel heat sink. *Int Commun Heat Mass Transfer*. 2011;38(1):63–8. <https://doi.org/10.1016/j.icheatmasstransfer.2010.09.012>.
 168. Xie G, Chen Z, Sunden B, Zhang W. Comparative study of the flow and thermal performance of liquid-cooling parallel-flow and counter-flow double-layer wavy microchannel heat sinks. *Numeri Heat Transf A Appl*. 2013;64(1):30–55. <https://doi.org/10.1080/10407782.2013.773811>.
 169. Sakanova A, Zhao J, Tseng KJ. Investigation on the influence of nanofluids in wavy microchannel heat sink. *IEEE Trans Compon Pack Manuf Technol*. 2015;5(7):956–70. <https://doi.org/10.1109/TCPMT.2015.2441114>.
 170. Chiam ZL, Lee PS, Singh PK, Mou N. Investigation of fluid flow and heat transfer in wavy micro-channels with alternating secondary branches. *Int J Heat Mass Transf*. 2016;101:1316–30. <https://doi.org/10.1016/j.ijheatmasstransfer.2016.05.097>.
 171. Pandey VK, Negi VPS, Ranganayakulu C. Numerical validation of straight microchannel heat exchanger and its performance comparison with wavy channel. *SSRN Electron J*. 2023. <https://doi.org/10.2139/SSRN.4380261>.
 172. Sui Y, Teo CJ, Lee PS. Direct numerical simulation of fluid flow and heat transfer in periodic wavy channels with rectangular cross-sections. *Int J Heat Mass Transf*. 2012;55(1–3):73–88. <https://doi.org/10.1016/j.ijheatmasstransfer.2011.08.041>.
 173. Xie G, Liu J, Liu Y, Sunden B, Zhang W. Comparative study of thermal performance of longitudinal and transversal-wavy microchannel heat sinks for electronic cooling. *J Electron Pack Trans ASME*. 2013;135(2):1–9. <https://doi.org/10.1115/1.4023530>.
 174. Lu H, Gong L, Xu M. Thermal performance of microchannels with dimples for electronics cooling. In *ASME 2013 4th International Conference on Micro/Nanoscale Heat and Mass Transfer, MNHMT 2013*, vol. 1(7), pp. 1029–1035; 2013. <https://doi.org/10.1115/MNHMT2013-22198>.
 175. Gong L, Kota K, Tao W, Joshi Y. Parametric numerical study of flow and heat transfer in microchannels with wavy walls. In: *ASME International Mechanical Engineering Congress and Exposition, Proceedings (IMECE)*, vol 7(A,B), pp. 1365–1373; 2010. <https://doi.org/10.1115/IMECE2010-40788>.
 176. Sakanova A, Keian CC, Zhao J. Performance improvements of microchannel heat sink using wavy channel and nanofluids. *Int J Heat Mass Transf*. 2015;89:59–74. <https://doi.org/10.1016/j.ijheatmasstransfer.2015.05.033>.
 177. Wang G, Qian N, Ding G. Heat transfer enhancement in microchannel heat sink with bidirectional rib. *Int J Heat Mass Transf*. 2019;136:597–609. <https://doi.org/10.1016/j.ijheatmasstransfer.2019.02.018>.
 178. Chai L, Wang L. Thermal-hydraulic performance of interrupted microchannel heat sinks with different rib geometries in transverse microchambers. *Int J Therm Sci*. 2018;127:201–12. <https://doi.org/10.1016/j.ijthermalsci.2018.01.029>.
 179. Chai L, Xia GD, Wang HS. Parametric study on thermal and hydraulic characteristics of laminar flow in microchannel heat sink with fan-shaped ribs on sidewalls—Part 1: heat transfer. *Int J Heat Mass Transf*. 2016;97:1069–80. <https://doi.org/10.1016/j.ijheatmasstransfer.2016.02.077>.
 180. Desrues T, Marty P, Fourmigué JF. Numerical prediction of heat transfer and pressure drop in three-dimensional channels with alternated opposed ribs. *Appl Therm Eng*. 2012;45–46:52–63. <https://doi.org/10.1016/j.applthermaleng.2012.03.013>.
 181. Chai L, Wang L, Bai X. Thermohydraulic performance of microchannel heat sinks with triangular ribs on sidewalls—Part 2: average fluid flow and heat transfer characteristics. *Int J Heat Mass Transf*. 2019;128:634–48. <https://doi.org/10.1016/j.ijheatmasstransfer.2018.09.027>.
 182. Derakhshanpour K, Kamali R, Eslami M. Effect of rib shape and fillet radius on thermal-hydrodynamic performance of microchannel heat sinks: A CFD study. *Int Commun Heat Mass Transfer*. 2020;119:104928. <https://doi.org/10.1016/j.icheatmasstransfer.2020.104928>.
 183. Gravndyan Q, et al. The effect of aspect ratios of rib on the heat transfer and laminar water/TiO₂ nanofluid flow in a two-dimensional rectangular microchannel. *J Mol Liq*. 2017;236:254–65. <https://doi.org/10.1016/j.molliq.2017.04.030>.
 184. Ghani IA, Kamaruzaman N, Sidik NAC. Heat transfer augmentation in a microchannel heat sink with sinusoidal cavities and rectangular ribs. *Int J Heat Mass Transf*. 2017;108:1969–81. <https://doi.org/10.1016/j.ijheatmasstransfer.2017.01.046>.
 185. Xia G, Zhai Y, Cui Z. Numerical investigation of thermal enhancement in a micro heat sink with fan-shaped reentrant cavities and internal ribs. *Appl Therm Eng*. 2013;58(1–2):52–60. <https://doi.org/10.1016/j.applthermaleng.2013.04.005>.
 186. Li YF, Xia GD, Ma DD, Jia YT, Wang J. Characteristics of laminar flow and heat transfer in microchannel heat sink with triangular cavities and rectangular ribs. *Int J Heat Mass Transf*.

- 2016;98:17–28. <https://doi.org/10.1016/j.ijheatmasstransfer.2016.03.022>.
187. Zhu Q, et al. Characteristics of heat transfer and fluid flow in microchannel heat sinks with rectangular grooves and different shaped ribs. *Alex Eng J.* 2020;59(6):4593–609. <https://doi.org/10.1016/j.aej.2020.08.014>.
 188. Wang G, Niu D, Xie F, Wang Y, Zhao X, Ding G. Experimental and numerical investigation of a microchannel heat sink (MCHS) with micro-scale ribs and grooves for chip cooling. *Appl Therm Eng.* 2015;85:61–70. <https://doi.org/10.1016/j.applthermaleng.2015.04.009>.
 189. Li F, Ma Q, Xin G, Zhang J, Wang X. Heat transfer and flow characteristics of microchannels with solid and porous ribs. *Appl Therm Eng.* 2020;178:115639. <https://doi.org/10.1016/j.applthermaleng.2020.115639>.
 190. Wang J, et al. Simulation of hybrid nanofluid flow within a microchannel heat sink considering porous media analyzing CPU stability. *J Pet Sci Eng.* 2022;208:109734. <https://doi.org/10.1016/j.petrol.2021.109734>.
 191. Li C, Li X, Huang H, Zheng Y. Hydrothermal performance analysis of microchannel heat sink with embedded module with ribs and pin-fins. *Appl Therm Eng.* 2023;225:120167. <https://doi.org/10.1016/j.applthermaleng.2023.120167>.
 192. Polat ME, Ulger F, Cadirci S. Multi-objective optimization and performance assessment of microchannel heat sinks with micro pin-fins. *Int J Thermal Sci.* 2022;174:107432. <https://doi.org/10.1016/j.ijthermalsci.2021.107432>.
 193. Zhang F, Wu B, Du B. Heat transfer optimization based on finned microchannel heat sink. *Int J Thermal Sci.* 2022;172:107357. <https://doi.org/10.1016/j.ijthermalsci.2021.107357>.
 194. Ghani IA, et al. Heat transfer enhancement in microchannel heat sink using hybrid technique of ribs and secondary channels. *Int J Heat Mass Transf.* 2017;114:640–55. <https://doi.org/10.1016/j.ijheatmasstransfer.2017.06.103>.
 195. Wang G, Chen T, Tian M, Ding G. Fluid and heat transfer characteristics of microchannel heat sink with truncated rib on sidewall. *Int J Heat Mass Transf.* 2020;148:119142. <https://doi.org/10.1016/j.ijheatmasstransfer.2019.119142>.
 196. Wang GL, Yang DW, Wang Y, Niu D, Zhao XL, Ding GF. Heat transfer and friction characteristics of the microfluidic heat sink with variously-shaped ribs for chip cooling. *Sensors (Switzerland).* 2015;15(4):9547–62. <https://doi.org/10.3390/s150409547>.
 197. Chai L, Xia GD, Wang HS. Numerical study of laminar flow and heat transfer in microchannel heat sink with offset ribs on sidewalls. *Appl Therm Eng.* 2016;92:32–41. <https://doi.org/10.1016/j.applthermaleng.2015.09.071>.
 198. Derakhshanpour K, Kamali R, Eslami M. Improving performance of single and double-layered microchannel heat sinks by cylindrical ribs: a numerical investigation of geometric parameters. *Int Commun Heat Mass Transfer.* 2021;126:105440. <https://doi.org/10.1016/j.icheatmasstransfer.2021.105440>.
 199. Zhai YL, Xia GD, Liu XF, Li YF. Heat transfer in the microchannels with fan-shaped reentrant cavities and different ribs based on field synergy principle and entropy generation analysis. *Int J Heat Mass Transf.* 2014;68:224–33. <https://doi.org/10.1016/j.ijheatmasstransfer.2013.08.086>.
 200. Datta A, Sharma V, Sanyal D, Das P. A conjugate heat transfer analysis of performance for rectangular microchannel with trapezoidal cavities and ribs. *Int J Therm Sci.* 2019;138:425–46. <https://doi.org/10.1016/j.ijthermalsci.2018.12.020>.
 201. Owhaib W, Palm B. Experimental investigation of single-phase convective heat transfer in circular microchannels. *Exp Therm Fluid Sci.* 2004;28(2–3):105–10. [https://doi.org/10.1016/S0894-1777\(03\)00028-1](https://doi.org/10.1016/S0894-1777(03)00028-1).
 202. Mokrani O, Bourouga B, Castelain C, Peerhossaini H. Fluid flow and convective heat transfer in flat microchannels. *Int J Heat Mass Transf.* 2009;52(5–6):1337–52. <https://doi.org/10.1016/j.ijheatmasstransfer.2008.08.022>.
 203. Naphon P, Khonseur O. Study on the convective heat transfer and pressure drop in the micro-channel heat sink. *Int Commun Heat Mass Transfer.* 2009;36(1):39–44. <https://doi.org/10.1016/j.icheatmasstransfer.2008.09.001>.
 204. Kang SW, Chen YT, Chang GS. The manufacture and test of (110) orientated silicon based micro heat exchanger. *Tamkang J Sci Eng.* 2002;5(3):129–36.
 205. Sabahi Namini A, Dilawary SAA, Motallebzadeh A, Shahedi Asl M. Effect of TiB₂ addition on the elevated temperature tribological behavior of spark plasma sintered Ti matrix composite. *Compos B Eng.* 2019;172:271–80. <https://doi.org/10.1016/j.compositesb.2019.05.073>.
 206. Sabahi Namini A, Azadbeh M, Shahedi Asl M. Effects of in-situ formed TiB whiskers on microstructure and mechanical properties of spark plasma sintered Ti-B₄C and Ti-TiB₂ composites. *Sci Iran.* 2018;25(2):762–71. <https://doi.org/10.24200/sci.2017.4499>.
 207. Traverso A, Massardo AF, Scarpellini R. Externally fired micro-gas turbine: modelling and experimental performance. *Appl Therm Eng.* 2006;26(16):1935–41. <https://doi.org/10.1016/j.applthermaleng.2006.01.013>.
 208. Al-attab KA, Zainal ZA. Performance of high-temperature heat exchangers in biomass fuel powered externally fired gas turbine systems. *Renew Energy.* 2010;35(5):913–20. <https://doi.org/10.1016/j.renene.2009.11.038>.
 209. Shahedi Asl M, Nayebi B, Shokouhimehr M. TEM characterization of spark plasma sintered ZrB₂-SiC-graphene nanocomposite. *Ceram Int.* 2018;44(13):15269–73. <https://doi.org/10.1016/j.ceramint.2018.05.170>.
 210. Akhlaghi M, Tayebifard SA, Salahi E, Shahedi Asl M. Spark plasma sintering of TiAl-Ti₃AlC₂ composite. *Ceram Int.* 2018;44(17):21759–64. <https://doi.org/10.1016/j.ceramint.2018.08.272>.
 211. Shahedi Asl M, Nayebi B, Ahmadi Z, Parvizi S, Shokouhimehr M. A novel ZrB₂-VB₂-ZrC composite fabricated by reactive spark plasma sintering. *Mater Sci Eng A.* 2018;731:131–9. <https://doi.org/10.1016/j.msea.2018.06.008>.
 212. Mohammadpour B, Ahmadi Z, Shokouhimehr M, Shahedi Asl M. Spark plasma sintering of Al-doped ZrB₂-SiC composite. *Ceram Int.* 2019;45(4):4262–7. <https://doi.org/10.1016/j.ceramint.2018.11.098>.
 213. Shahedi Asl M, Ahmadi Z, Sabahi Namini A, Babapour A, Motallebzadeh A. Spark plasma sintering of TiC-SiCw ceramics. *Ceram Int.* 2019;45(16):19808–21. <https://doi.org/10.1016/j.ceramint.2019.06.236>.
 214. Nekahi S, Vaferi K, Vajdi M, Sadegh Moghanlou F, Shahedi Asl M, Shokouhimehr M. A numerical approach to the heat transfer and thermal stress in a gas turbine stator blade made of HfB₂. *Ceram Int.* 2019;45(18):24060–24069. doi: <https://doi.org/10.1016/j.ceramint.2019.08.112>.
 215. Nakamori F, Ohishi Y, Muta H, Kurosaki K, Fukumoto KI, Yamanaka S. Mechanical and thermal properties of bulk ZrB₂. *J Nucl Mater.* 2015;467:612–7. <https://doi.org/10.1016/j.jnucmat.2015.10.024>.
 216. Zhu S, Fahrenholtz WG, Hilmas GE. Influence of silicon carbide particle size on the microstructure and mechanical properties of zirconium diboride-silicon carbide ceramics. *J Eur Ceram Soc.* 2007;27(4):2077–83. <https://doi.org/10.1016/j.jeurceramsoc.2006.07.003>.
 217. Königshofer R et al. Solid-state properties of hot-pressed TiB₂ ceramics. *Int J Refract Metals Hard Mater.* 2005;23(4–6 SPEC. ISS):350–357. <https://doi.org/10.1016/j.ijrmhm.2005.05.006>.
 218. Sarowar MT. Numerical analysis of a liquid metal cooled mini channel heat sink with five different ceramic substrates. *Ceram*

- Int. 2021;47(1):214–25. <https://doi.org/10.1016/j.ceramint.2020.08.124>.
219. Xie SH, Zhu BK, Li JB, Wei XZ, Xu ZK. Preparation and properties of polyimide/aluminum nitride composites. *Polym Test*. 2004;23(7):797–801. <https://doi.org/10.1016/j.polymertesting.2004.03.005>.
 220. Akishin GP, et al. Thermal conductivity of beryllium oxide ceramic. *Refract Ind Ceram*. 2009;50(6):465–8. <https://doi.org/10.1007/s11148-010-9239-z>.
 221. Alm B, Imke U, Knitter R, Schygulla U, Zimmermann S. Testing and simulation of ceramic micro heat exchangers. *Chem Eng J*. 2008;135(SUPPL. 1). <https://doi.org/10.1016/j.cej.2007.07.005>.
 222. Fend T, et al. Experimental investigation of compact silicon carbide heat exchangers for high temperatures. *Int J Heat Mass Transf*. 2011;54(19–20):4175–81. <https://doi.org/10.1016/j.ijheatmasstransfer.2011.05.028>.
 223. PEB de Mello, Villanueva HHS, Scuotto S, Donato GHB, Ortega FdS. Heat transfer, pressure drop and structural analysis of a finned plate ceramic heat exchanger. *Energy*. 2017;120:597–607. <https://doi.org/10.1016/j.energy.2016.11.113>
 224. Lewinsohn C. High-efficiency, ceramic microchannel heat exchangers. *Am Ceram Soc Bull*. 2015;95(4):26–31.
 225. Carman BG, Kapat JS, Chow LC, An L. Impact of a ceramic microchannel heat exchanger on a micro turbine. *American Society of Mechanical Engineers, International Gas Turbine Institute, Turbo Expo (Publication) IGTI*, vol. 1, pp. 1053–1060, 2002. <https://doi.org/10.1115/GT2002-30544>.
 226. Ponyavin V, Chen Y, Mohamed T, Trabia M, Hechanova AE, Wilson M. Design of a compact ceramic high-temperature heat exchanger and chemical decomposer for hydrogen production. *Heat Transfer Eng*. 2012;33(10):853–70. <https://doi.org/10.1080/01457632.2012.654446>.
 227. Monteiro DB, de Mello PEB. Thermal performance and pressure drop in a ceramic heat exchanger evaluated using CFD simulations. *Energy*. 2012;45(1):489–96. <https://doi.org/10.1016/j.energy.2012.02.012>.
 228. Nekahi S, et al. TiB₂–SiC-based ceramics as alternative efficient micro heat exchangers. *Ceram Int*. 2019;45(15):19060–7. <https://doi.org/10.1016/j.ceramint.2019.06.150>.
 229. Fattahi M, Vaferi K, Vajdi M, Sadegh Moghanlou F, Sabahi Namini A, Shahedi Asl M. Aluminum nitride as an alternative ceramic for fabrication of microchannel heat exchangers: a numerical study. *Ceram Int*. 2020;46(8):11647–11657. <https://doi.org/10.1016/j.ceramint.2020.01.195>
 230. Vajdi M, Sadegh Moghanlou F, Ranjbarpour Niari E, Shahedi Asl M, Shokouhimehr M. Heat transfer and pressure drop in a ZrB₂ microchannel heat sink: A numerical approach. *Ceram Int*. 2020;46(2):1730–1735. <https://doi.org/10.1016/j.ceramint.2019.09.146>
 231. Li X et al. Design and modeling of a multiscale porous ceramic heat exchanger for high temperature applications with ultrahigh power density. *Int J Heat Mass Transf*. 2022;194:122996. <https://doi.org/10.1016/J.IJHEATMASSTRANSFER.2022.122996>.
 232. Vaferi K, et al. Numerical simulation of cooling performance in microchannel heat sinks made of AlN ceramics. *Microsyst Technol*. 2023;29(1):141–56. <https://doi.org/10.1007/S00542-022-05400-X/FIGURES/17>.
 233. Cao Y, El-Shorbagy MA, Sharma K, Aly AA, Felemban BF. Role of beryllium oxide on the thermal efficiency of microchannel heat exchanger with an optimum fin structure. *Ceram Int*. 2022;48(7):9973–86. <https://doi.org/10.1016/J.CERAMINT.2021.12.204>.
 234. Cao Y et al. Thermo-hydraulic performance in ceramic-made microchannel heat sinks with an optimum fin geometry. *Case Stud Thermal Eng*. 2022;36:102230. <https://doi.org/10.1016/J.CSITE.2022.102230>.
 235. Dwivedi A, Khan MM, Pali HS. Numerical analysis of micro-channel heat sink composed of SiC and CNT reinforced ZrB₂ composites. *J Eng Res*. 2022. <https://doi.org/10.36909/JER.18359>.
 236. Prajapati YK. Influence of fin height on heat transfer and fluid flow characteristics of rectangular microchannel heat sink. *Int J Heat Mass Transf*. 2019;137:1041–52. <https://doi.org/10.1016/j.ijheatmasstransfer.2019.04.012>.
 237. Wu Y et al. Enhanced thermal and mechanical performance of 3D architected micro-channel heat exchangers. *Heliyon*. 2023;9(3):e13902. <https://doi.org/10.1016/J.HELIYON.2023.E13902>.
 238. Kumar K, Kumar P. Effect of groove depth on hydrothermal characteristics of the rectangular microchannel heat sink. *Int J Thermal Sci*. 2021;161:106730. <https://doi.org/10.1016/j.ijthermalsci.2020.106730>.
 239. Ma H, Duan Z, Ning X, Su L. Numerical investigation on heat transfer behavior of thermally developing flow inside rectangular microchannels. *Case Stud Thermal Eng*. 2021;24:100856. <https://doi.org/10.1016/j.csite.2021.100856>.
 240. Lan Y, Feng Z, Huang K, Zhang J, Hu Z. Effects of truncated and offset pin-fins on hydrothermal performance and entropy generation in a rectangular microchannel heat sink with variable fluid properties. *Int Commun Heat Mass Transf*. 2021;124:105258. <https://doi.org/10.1016/j.icheatmasstransfer.2021.105258>.
 241. Kose HA, Yildizeli A, Cadirci S. Parametric study and optimization of microchannel heat sinks with various shapes. *Appl Therm Eng*. 2022;211:118368. <https://doi.org/10.1016/J.APPLTHERMALENG.2022.118368>.
 242. Fani B, Abbassi A, Kalteh M. Effect of nanoparticles size on thermal performance of nanofluid in a trapezoidal microchannel-heat-sink. *Int Commun Heat Mass Transfer*. 2013;45:155–61. <https://doi.org/10.1016/j.icheatmasstransfer.2013.04.003>.
 243. Weilin Q, Mohiuddin Mala G, Dongqing L. Pressure-driven water flows in trapezoidal silicon microchannels. *Int J Heat Mass Transf*. 2000;43(3):353–364. [https://doi.org/10.1016/S0017-9310\(99\)00148-9](https://doi.org/10.1016/S0017-9310(99)00148-9).
 244. Song J, Liu F, Sui Y, Jing D. Numerical studies on the hydraulic and thermal performances of trapezoidal microchannel heat sink. *Int J Thermal Sci*. 2021;161:106755. <https://doi.org/10.1016/j.ijthermalsci.2020.106755>.
 245. Ahmed HE, Ahmed MI. Optimum thermal design of triangular, trapezoidal and rectangular grooved microchannel heat sinks. *Int Commun Heat Mass Transfer*. 2015;66:47–57. <https://doi.org/10.1016/j.icheatmasstransfer.2015.05.009>.
 246. Mohammed HA, Bhaskaran G, Shuaib NH, Abu-Mulaweh HI. Influence of nanofluids on parallel flow square microchannel heat exchanger performance. *Int Commun Heat Mass Transfer*. 2011;38(1):1–9. <https://doi.org/10.1016/j.icheatmasstransfer.2010.09.007>.
 247. Zheng L, Zhang D, Xie Y, Xie G. Thermal performance of dimpled/protruded circular and annular microchannel tube heat sink. *J Taiwan Inst Chem Eng*. 2016;60:342–51. <https://doi.org/10.1016/j.jtice.2015.10.026>.
 248. Monavari A, Jamaati J, Bahiraei M. Thermohydraulic performance of a nanofluid in a microchannel heat sink: Use of different microchannels for change in process intensity. *J Taiwan Inst Chem Eng*. 2021;125:1–14. <https://doi.org/10.1016/j.jtice.2021.05.045>.
 249. Wang H, Chen Z, Gao J. Influence of geometric parameters on flow and heat transfer performance of micro-channel heat sinks. *Appl Therm Eng*. 2016;107:870–9. <https://doi.org/10.1016/j.applthermaleng.2016.07.039>.
 250. Tan P, Liu X, Cao B, Chen W, Feng J. Heat exchange mechanism analysis and structural parameter optimization for series-combined microchannel heat sinks. *Int J Thermal Sci*.

2023;187:108168. <https://doi.org/10.1016/J.IJTHEMALSCI.2023.108168>.

Publisher's Note Springer Nature remains neutral with regard to jurisdictional claims in published maps and institutional affiliations.

Springer Nature or its licensor (e.g. a society or other partner) holds exclusive rights to this article under a publishing agreement with the author(s) or other rightsholder(s); author self-archiving of the accepted manuscript version of this article is solely governed by the terms of such publishing agreement and applicable law.